Turkish Journal of Engineering & Environmental Sciences

http://journals.tubitak.gov.tr/engineering/

Research Article

Turkish J Eng Env Sci
(2014) 38: 11 – 40

doi:10.3906/muh-1304-24

Chemically treated kola nut pod as low-cost natural adsorbent for the removal of 2,4-dinitrophenol from synthetic wastewater: batch equilibrium, kinetic, and thermodynamic modelling studies

Samuel AGARRY*, Oladipupo OGUNLEYE
Department of Chemical Engineering, Biochemical and Bioenvironmental Engineering Laboratory,
Ladoke Akintola University of Technology, Ogbomoso, Nigeria

Received: 19.04.2013 • **Accepted:** 12.04.2014 • **Published Online:** 24.10.2014 • **Printed:** 21.11.2014

Abstract: The feasibility of using chemically treated kola nut pod to remove 2,4-dinitrophenol from its aqueous solutions under batch mode was investigated. The results showed that biosorption of 2,4-dinitrophenol was dependent on initial concentration, contact time, pH, biosorbent particle size, biosorbent dosage, and temperature. The batch equilibrium biosorption data were analyzed by 2 two-parameter (Langmuir and Freundlich) and 2 three-parameter (Redlich–Peterson and Sips) adsorption isotherm models using linear and nonlinear regression methods. The Sips isotherm equation employing the parameter sets derived using the HYBRID/MPSD/ARE errors provided the overall best model to describe the biosorption data of the 2,4-dinitrophenol-kola nut pod system. The maximum monolayer biosorption capacity (Q_{max}) was obtained to be 32.26 mg/g with linear regression and 30.10 mg/g with nonlinear regression. The biosorption kinetic data were fitted to 6 biosorption kinetic models using the linear regression method. The 6 kinetic models fitted well to the biosorption kinetic data; however, the pseudo-first-order kinetic model gave the best fit and the biosorption mechanism was controlled by film diffusion. The thermodynamic analysis indicates that the biosorption process was spontaneous, feasible, exothermic, and physical in nature. Thus, chemically modified kola nut pod has potential for application as an effective bioadsorbent for 2,4-dinitrophenol removal from wastewater.

Key words: Agricultural waste, biosorption isotherms, biosorption kinetics, kola-nut pod, thermodynamic properties, 2,4-dinitrophenol

1. Introduction

Phenolic compounds including nitrophenols are widely used in pharmaceutical, petrochemical, and other chemical manufacturing industries [1] and could also be found in the liquid waste effluents discharged from these industries. Nitrophenols are listed as priority toxic pollutants by the US Environmental Protection Agency [2]. These organic pollutants can enter our bodies through the lungs and their toxicity lies in the chemical reaction with protein in the bioplasm of the organism's cells, producing insoluble protein and resulting in the loss of activity of the cell and the restraining of microbial growth [3]. Thus, treatment of wastewater containing phenolic compounds has become inevitable before its being discharged into the environment in order to reduce its side effects on the environment and human health. There are many methods, such as oxidation, ion exchange, electrochemical oxidation, reverse osmosis, photocatalytic degradation, ultrafiltration, and adsorption

*Correspondence: seagarry@lautech.edu.ng

[4–8], that have been used for the removal of phenol and its derivatives. Among these technologies, adsorption is a well-established, powerful, and particularly effective process for the removal of hazardous inorganic and organic pollutants in industrial waste effluents and contaminated ground water [1].

A number of adsorption materials have been studied for their capacity to remove pollutants, including ion exchange resins, bentonite, zeolite [1,9,10], silica gel, activated carbon [7], and alginate [3]. Activated carbon is the most widely used adsorbent with high adsorption capacity for organic compounds, but its use is usually limited due to its high cost. Therefore, over the last few years a number of investigations have been carried out to utilize low-cost naturally occurring and efficient adsorbents such as wood, red mud, coconut shell, chitin, and sugarcane bagasse [11–13]. In recent years there has been increasing interest in utilizing agricultural by-products like tamarind fruit shell, orange peel, pine bark, and spent tea leaves as adsorbents for the removal of toxic metals and some organic pollutant from aqueous solutions [14–18].

Modeling is a valuable engineering tool in both design and operation of treatment plants. Furthermore, modeling of wastewater treatment plants can be used for process optimization and testing of control strategies in order to meet effluent quality requirements at a reasonable cost [1]. It also helps to develop a better understanding of the treatment processes and provides a significant potential for solving operational problems as well as reducing operational costs in specific treatment processes. Particularly, the development of kinetic models gives good insight into reaction mechanisms and describes several specific parameters for monitoring the system performance. So far, 2 isotherm models and 3 kinetic models have been successfully applied in various studies on adsorption and biosorption processes to determine the importance of the relationship between the design data and the experimental results [18–21].

Biosorption of pollutants such as heavy metals and organic chemicals from contaminated waters is a relatively new and promising area of exploitation of biomass wastes [22]. Biosorption is a cheap and environmentally safe alternative to the use of traditional adsorbents; hence, the suitability of a given biomass for this application needs careful evaluation [23]. Few investigations have been conducted to test the removal of nitrophenol from contaminated water and waste waters using adsorbents such as alginate, zeolite, bentonite, and magnesium-aluminum mixed oxide [1,3,24,25]. However, information on the use of kola nut pods as agricultural waste adsorbent for the removal of organic chemicals from contaminated water or waste waters is scarce.

Kola (a member of the family Sterculiaceae) is mostly produced in Africa and is cultivated to a large degree in Nigeria, but also in Ghana, the Ivory Coast, Brazil, and the West Indian Islands [26]. Annual production from these countries alone is in excess of 250,000 t, while the world production is about 300,000 t [27]. There are over 40 kola species, out of which *Cola nitida* and *Cola acuminata* are of major economic and social importance in Nigeria [28]. They are used industrially for the production of different types of soft drink flavors and wines and have found industrial usage in pharmaceuticals and confectionaries [29–31]. Nigeria produces 70% of the world's kola nut supply and consequently the bulk of kola nut pod is estimated at 210,000 t annually [29]. The kola nut pod, which is a by-product obtained from the processing of the nut, is widely used for animal feeding because of its high nutritive quality, but its adsorptive potential has not been fully explored in the treatment of contaminated water and wastewater.

Therefore, the objective of this study is to investigate the possibility and potential of using cellulose-based waste kola nut (*Cola acuminata*) pod as a novel ecofriendly low-cost biosorbent for the biosorption of 2,4-dinitrophenol (2,4-DNP) from aqueous solution. The effects of physical parameters such as initial 2,4-DNP concentration, particle size, pH, temperature, and biosorbent dosage on the biosorption process were investigated. Linear and nonlinear regression analysis was performed to determine biosorption isotherm models

parameters and 5 error functions were applied to evaluate, compare, and rank the feasibility of the applied isotherm models. The kinetics and thermodynamic parameters were also determined and evaluated.

2. Materials and methods

2.1. Preparation of synthetic wastewater sample

All the reagents used for the current investigation were of analytical grade from E. Merck Ltd., India. A stock solution was prepared by dissolving 1 g of 2,4-DNP (Sigma Aldrich, USA) in 1 L of sterilized deionized water. From this original stock solution, 5 working test solutions with various concentrations (100, 200, 300, 400, and 500 mg/L) were prepared by dilution with deionized water. Before mixing the adsorbent, the pH of each 2,4-DNP solution was adjusted to the required value by 0.1 M NaOH or 0.1 M HCl solution.

2.2. Kola nut pod preparation and characterization

The kola nut (*Cola acuminata*) pods used in this study were obtained from a local market located in Ogbomoso, Nigeria. The kola nut pods were rinsed with deionized water and sundried for 2 weeks. The sun-dried kola nut pods were again rinsed thoroughly with sterilized deionized water and dried in the oven for 12–24 h at 60 °C, after which they were ground and sieved to different particle sizes that ranged between 0.192 and 1.700 mm and were stored in sterilized closed glass bottles at ambient temperature prior to use as a biosorbent. The kola nut pods were characterized for specific surface area, true bulk density, apparent particle density, moisture content, and porosity. The specific surface area of the sorbent was determined using the iodine number sorption method [32]. The iodine number was determined according to the ASTM D4607-94 method [32]. The iodine number is defined as the milligrams of iodine adsorbed by 1.0 g of carbon when the iodine concentration of the filtrate is 0.02 mol L^{-1}. This method is based upon a 3-point isotherm. A standard iodine solution is treated with 3 different weights of kola nut pod under specified conditions. The experiment consists of treating the kola nut pod sample with 10.0 mL of 5% HCl. This mixture was boiled for 30 s and then cooled. Soon afterwards, 100.0 mL of 0.1 mol L^{-1} iodine solution was added to the mixture and stirred for 30 s. The resulting solution was filtered and 50.0 mL of the filtrate was titrated with 0.1 mol L^{-1} sodium thiosulfate, using starch as an indicator. The iodine amount adsorbed per gram of carbon (X/M) was plotted against the iodine concentration in the filtrate (C), using logarithmic axes (plot not shown). If the residual iodine concentration (C) is not within the range of 0.008 to 0.04 mol L^{-1}, the whole procedure should be repeated using different kola nut pod masses for each isotherm point. A least squares fitting regression was applied for the 3 points. The iodine number is the X/M value when the residual concentration (C) is 0.02 mol L^{-1}. The X/M and C values are calculated using Eqs. (1) and (2), respectively.

$$X/M = \frac{(M_1 \times 126.93 \times V_1) - [(V_1 + V_{HCL})/V_F] \times (M_{Na_2S_2O_3} \times 126.93) \times V_{Na_2S_2O_3})}{M_{KP}} \quad (1)$$

$$C = M_{Na_2S_2O_3} \times V_{Na_2S_2O_3} \quad (2)$$

Here, M_1 is the iodine solution molarity, V_1 is the added volume of iodine solution, V_{HCL} is the added volume of 5% HCl, V_F is the filtrate volume used in titration, $M_{Na_2S_2O_3}$ is the sodium thiosulfate solution molarity, $V_{Na_2S_2O_3}$ is the consumed volume of sodium thiosulfate solution, and M_{KP} is the mass of kola nut pod.

Other physical parameters such as moisture content, specific gravity, true bulk density, particle density, and porosity were also determined using standard methods [33,34]. The physical characteristics of kola nut pods are given in Table 1.

Table 1. Physical characteristics of kola nut pod.

Parameters	Value
Moisture content (%)	11.29 ± 0.30
Specific surface area (A_S), m^2/g	224.8 ± 0.6
Specific gravity	0.860 ± 0.02
True bulk density (ρ_s), g/cm^3	0.340 ± 0.04
Apparent particle density (ρ_p), g/cm^3	0.227 ± 0.02
Porosity (ε) = $[1 - (\rho_p/\rho_s)]$	0.66 ± 0.02

Each value is a mean of 3 replicates ± standard deviation.

2.3. Pretreatment of kola nut pod

The kola nut pods were pretreated with chemical solvent to increase the 2,4-DNP uptake efficiency. For this purpose, 100 g of the kola nut pod was treated with 1000 mL of 1 M phosphoric acid (H_3PO_4) for 24 h and then kept in a water bath (70 °C) for 30 min. It was later cooled and neutralized with 500 mL of 1 M NaOH. The filtrates were separated and dried in the oven at 60 °C for 12–24 h. The pretreated kola nut pods were used as biosorbent for the study.

2.4. Batch biosorption equilibrium and kinetic studies

The batch biosorption tests were carried out in a glass-stoppered, Erlenmeyer flask with 100 mL of working volume and an initial concentration of 100 mg/L of 2,4-DNP. A weighed amount (2.0 g) of biosorbent was added to the solution. The flasks were agitated for 100 min on a magnetic stirrer at ambient temperature (25 ± 2 °C). The influence of initial 2,4-DNP concentration (100, 200, 300, 400, 500 mg/L), contact time (20, 40, 60, 80, 100 min), particle size (0.192, 0.25, 0.390, 0.780, 1.700 mm), pH (4, 5, 6, 7, 8), biosorbent dose (2, 4, 6, 8, 10 g/100 mL), and temperature (25, 30, 35, 40, 45 °C) was evaluated. Samples were collected from the flasks at predetermined time intervals for analyzing the residual 2,4-DNP concentration in the solution. Prior to analysis, samples were centrifuged to separate biosorbent from the sorbate and minimize interferences. At time t = 0 and equilibrium, the 2,4-DNP concentrations were determined using a UV-spectrophotometer at an absorbance wavelength of 320 nm. The amount of biosorption at equilibrium, q_e (mg/g), was calculated according to Eq. (3) [13]:

$$q_e = \frac{(C_o - C_e)V}{W}, \tag{3}$$

where C_o and C_e (mg/L) are the initial and final (equilibrium) concentrations of 2,4-DNP in waste water. V (mL) is the volume of the waste water and W (g) is the mass of dry biosorbent used.

The procedures of kinetic studies were basically identical to those of batch equilibrium studies.

The amount of 2,4-DNP sorbed at time t, q_t, was calculated according to Eq. (4) [35]:

$$q_t = \frac{(C_o - C_t)V}{W}, \tag{4}$$

where C_t is the concentration of 2,4-DNP in waste water at time t. The percentage of 2,4-DNP removal was calculated using Eq. (5) [36].

$$\text{Removal } (\%) = \frac{C_o - C_t}{C_o} \times 100 \tag{5}$$

3. Results and discussion

3.1. Effect of initial concentration and contact time

The rate of biosorption is a function of the initial concentration of the sorbate, which makes it an important factor to be considered for effective biosorption. Figures 1a and 1b respectively show the effects of contact time and initial concentration on 2,4-DNP removal by chemically treated kola nut pods. The removal rate was rapid initially and then gradually decreased to attain an equilibrium time beyond which there was no significant increase in the rate of removal. The equilibrium was nearly reached after 60 min for 5 different initial 2,4-DNP concentrations (Figure 1a). Hence, in the present work, 60 min was chosen as the equilibrium time. The fast biosorption rate at the initial stage may be due to an increased availability in the number of active binding sites on the biosorbent surface. The biosorption rapidly occurs and is normally controlled by the diffusion process from the bulk to the surface. However, at the later stage, the biosorption is likely an attachment-controlled process due to fewer available biosorption sites. Similar findings for nitrophenol adsorption onto other adsorbents were reported by other investigators [1,37] as well as for chlorophenols [36,38,39]. Furthermore, the biosorption capacity at equilibrium increased with an increase in initial 2,4-DNP concentration (Figure 1a). This is due to the increasing concentration gradient, which acts as an increasing driving force to overcome the resistances to mass transfer of 2,4-DNP between the aqueous phase and the solid phase [40]. Similar results were obtained in the adsorption of 4-nitrophenol onto fly ash [1,41,42]. However, the percentage removal of 2,4-DNP decreased with the increment of the initial 2,4-DNP concentration (Figure 1b). This observation is due to the fact that all biosorbents have a limited number of active sites and at a certain concentration the active sites become saturated [43].

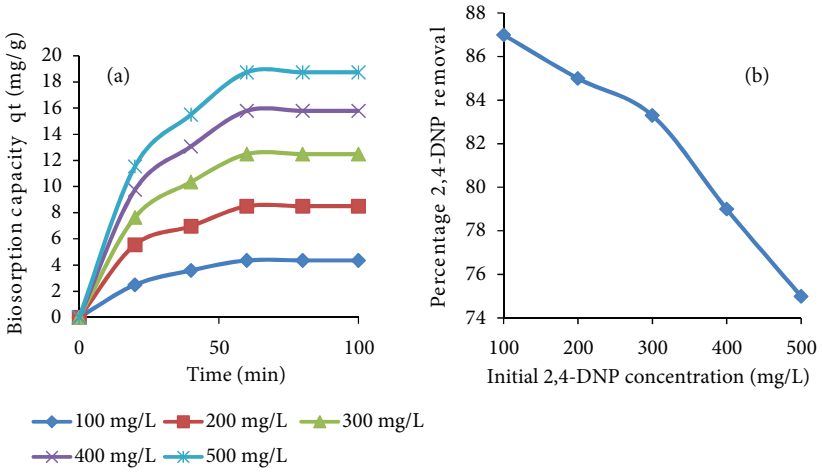

Figure 1. Effect of initial concentration and contact time on (a) biosorption capacity of chemically treated kola nut pod and (b) percentage 2,4-DNP removal by chemically treated kola nut pod.

3.2. Effect of biosorbent particle size

Figures 2a and 2b respectively show the effect of biosorbent particle size on the biosorption of 2,4-DNP by chemically treated kola nut pods. It is seen that the biosorption capacity of kola nut pods increased with decrease in particle size diameter; thus, the removal of 2,4-DNP increases as the particle size diameter decreases (Figure 2a). Similar observations have been reported for adsorption of unsubstituted phenol [44] and the biosorption of 2,6-dichlorophenol [39]. Decrease in particle size increases the percentage removal (Figure 2b)

due to increase in surface area as well as micropore volume [45]. Smaller particle size means more interior surface and micropore volume, and hence the area of active sites for adsorption will be greater. Additionally, for larger particles, the diffusion resistance to mass transfer is higher and most of the internal surfaces of the particle may not be utilized for adsorption; consequently, the amount of 2,4-DNP adsorbed is small [44,46].

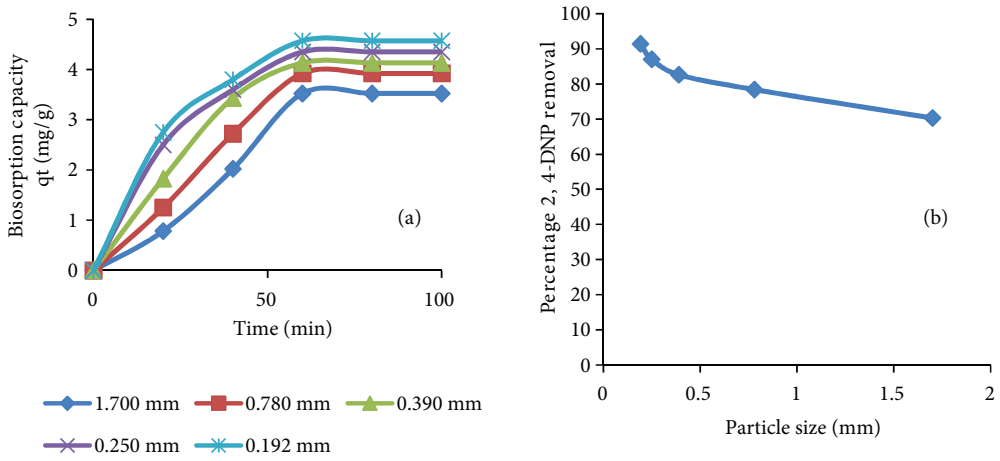

Figure 2. Effect of particle size on (a) biosorption capacity of chemically treated kola nut pod and (b) percentage 2,4-DNP removal by chemically treated kola nut pod.

3.3. Effect of pH

The removal of pollutant from waste water by adsorption is highly dependent on the waste water pH, which affects the surface charge of the biosorbent and the degree of ionization of the sorbate (pollutant). The effect of solution pH on 2,4-DNP biosorption was studied using 2 g of chemically treated kola nut pods and 100 mg/L 2,4-DNP at ambient temperature (25 °C). The range of pH was adjusted between 4 and 8 to study the effect of pH on the percentage removal of 2,4-DNP (Figures 3a and 3b). As can be seen from Figure 3a, it is evident that increasing the pH of the synthetic waste water generally serves to increase the biosorption capacity, with a significant enhancement in the biosorption process occurring as the pH increased from 4 to 8. It was found that the biosorption of 2,4-DNP increased as the pH of the synthetic waste water was increased (Figure 3b). This observation is consistent with previous studies on the adsorption of p-nitrophenol onto palm oil fuel ash [47], fly ash [40], activated jute stick char [48], and clay [49]. This increase in 2,4-DNP biosorption may be due to the presence of the nitro group in the benzene ring [49].

In this present experiment the percent removal of 2,4-DNP by biosorption was at maximum between pH 7 and 8. The pH of waste water or medium controls the electrostatic interactions between the biosorbent and the sorbate. The surface nature of a biosorbent depends not only on the surface functional groups but also on the isoelectric point (pH_{IEP}) or point of zero charge (pH_{PZC}) of the biosorbent [50]. At a lower pH (acidic pH), the total or external surface charges on the biosorbent are positive. Thus, lower biosorption of 2,4-DNP took place at lower pH values. The lowest 2,4-DNP biosorption was observed at pH 4. Cationic biosorption is favored at $pH > pH_{PZC}$ and anionic biosorption is favored at $pH < pH_{PZC}$ [50]. When the pH value was increased, the surface of the biosorbent was more negatively charged; therefore, the biosorption of 2,4-DNP with positive charge reached an optimum at a pH value that lay between 7 and 8. In other words, the biosorption capacity increased with increase in pH and the maximum biosorption capacity occurred at pH 7.

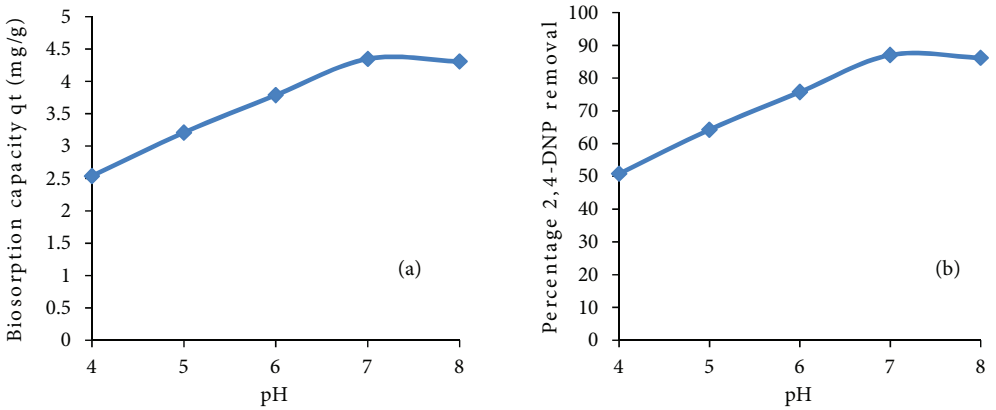

Figure 3. Effect of solution pH on (a) biosorption capacity of chemically treated kola nut pod and (b) percentage 2,4-DNP removal by chemically treated kola nut pod.

3.4. Effect of temperature

The biosorption of 2,4-DNP on chemically treated kola nut pods was investigated as a function of temperature and maximum removal of 2,4-DNP was obtained at 25 °C (Figures 4a and 4b). The biosorption capacity decreased with the rise in temperature from 25 to 45 °C (Figure 4a). This is mainly due to the decreased surface activity, suggesting that biosorption between 2,4-DNP and chemically treated kola nut pods was an exothermic process. Similar observations were reported for the adsorption of 4-nitrophenol onto fly ash [1,43]. The percentage removal of 2,4-DNP decreased with the increment of the solution temperature (Figure 4b).

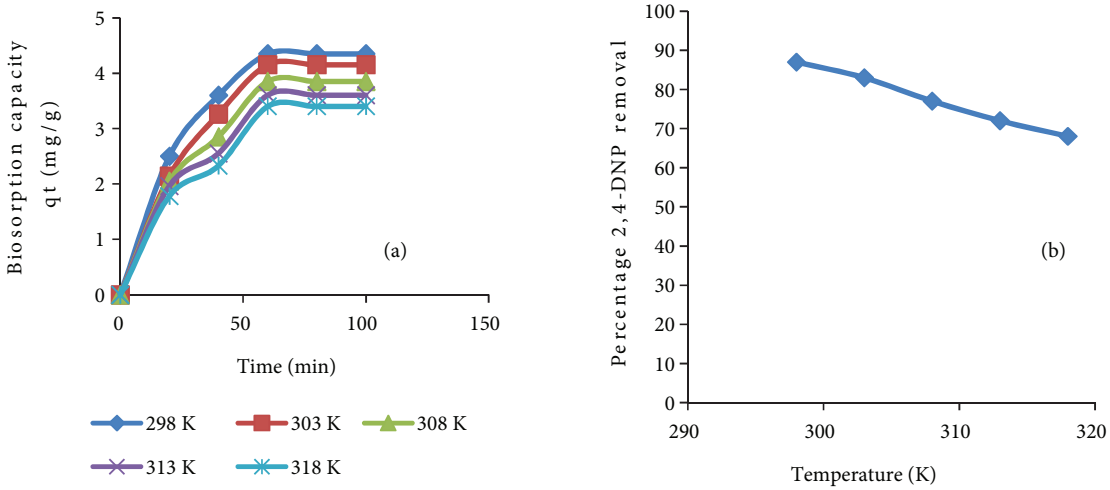

Figure 4. Effect of temperature on (a) biosorption capacity of chemically treated kola nut pod and (b) percentage 2,4-DNP removal by chemically treated kola nut pod.

3.5. Effect of biosorbent dosage

In this study, 5 different biosorbent dosages were selected, ranging from 2 to 10 g, while the 2,4-DNP concentration was fixed at 100 mg/L. The results are presented in Figures 5a and 5b. As the biosorbent dosage was increased from 2 to 10 g, the biosorption capacity reduced from 4.35 to 0.929 mg/g (Figure 5a). This may

be due to the decrease in total biosorption surface area available to 2,4-DNP, resulting from overlap or aggregation of biosorption sites [51,52]. Similar observations have been reported [18,53,54]. Thus, with increasing biosorbent mass, the amount of 2,4-DNP sorbed onto unit mass of biosorbent is reduced, causing a decrease in q value with increasing biosorbent mass concentration. However, the percentage of 2,4-DNP removal showed an opposite trend. It was observed that percentage of 2,4-DNP removal increased with increase in biosorbent dose (Figure 5b). This kind of a trend is mostly attributed to an increase in the biosorptive surface area and the availability of more active binding sites on the surface of the adsorbent [54,55]. Furthermore, maximum 2,4-DNP percentage removal (93%) was recorded between 8 and 10.0 g of chemically treated kola nut pods.

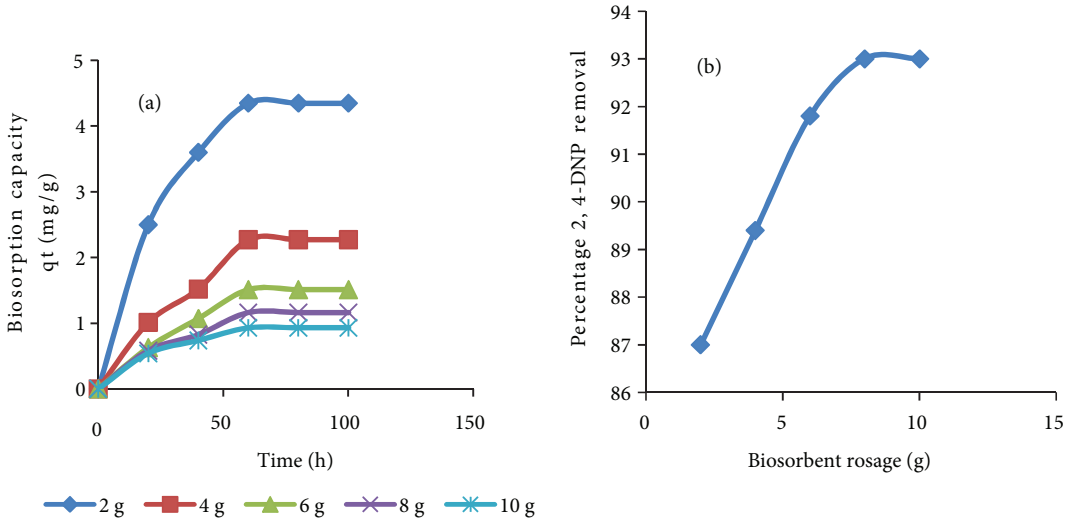

Figure 5. Effect of biosorbent dosage on (a) biosorption capacity of chemically treated kola nut pod and (b) percentage 2,4-DNP removal by chemically treated kola nut pod.

3.6. Biosorption isotherms

An adsorption/biosorption isotherm represents the equilibrium relationship between the adsorbate concentration in the liquid phase and that on the adsorbents' surface at a given condition. A number of 2- or 3-parameter adsorption isotherm models have been developed to describe adsorption equilibrium relationships. In the present study, 2- and 3-parameter models of Langmuir, Freundlich, Redlich–Peterson, and Sips were used to describe the equilibrium data in a wide variation of concentrations. The simplest method to determine isotherm constants for 2-parameter isotherms is to transform the isotherm variables so that the equation is converted to a linear form and then to apply linear regression. Although linear analysis is not possible for 3- and 4-parameter isotherms, a trial-and-error procedure has usually been applied to a pseudo-linear form of the isotherm to obtain values for the isotherm constants [56]. The transformations of nonlinear isotherm equations to linear forms implicitly alter their error structure and may also violate the error variance and normality assumptions of standard least squares [57]. In recent times, due to the inherent bias resulting from linearization, alternative isotherm parameter sets have been determined using a nonlinear optimization regression method. This provides a mathematically rigorous method for determining isotherm parameters using the original form of the isotherm equation [58]. The optimization procedure requires the selection of an error function in order to evaluate the fit of the isotherm to the experimental equilibrium data. Since the choice of error function can affect the

parameters derived, 5 different error functions were examined and in each case a set of isotherm parameters were determined by minimizing the respective error function across the concentration range studied using the Solver add-in with Microsoft Excel. The error functions employed are shown below [59,60].

Sum of the square of the error (ERRSQ):

$$ERRSQ = \sum (q_e^{\mathrm{mod}} - q_e^{\mathrm{exp}})^2 \tag{6}$$

Hybrid fractional function error (HYBRID):

$$HYBRID = \frac{100}{p-n} \sum_{i=1}^{p} \left[\frac{(q_e^{\mathrm{exp}} - q_e^{\mathrm{mod}})^2}{q_e^{\mathrm{exp}}} \right]_i \tag{7}$$

Marquardt's percent standard deviation (MPSD):

$$MPSD = 100 \left(\sqrt{\frac{1}{p-n} \sum_{i=1}^{p} \left[\frac{(q_e^{\mathrm{exp}} - q_e^{\mathrm{mod}})^2}{q_e^{\mathrm{exp}}} \right]_i} \right) \tag{8}$$

Average relative error (ARE):

$$ARE = \frac{100}{p} \sum_{i=1}^{p} \left[\frac{(q_e^{\mathrm{exp}} - q_e^{\mathrm{mod}})^2}{q_e^{\mathrm{exp}}} \right]_i \tag{9}$$

Sum of absolute error (EABS):

$$EABS = \sum_{i=1}^{p} (q_e^{\mathrm{exp}} - q_e^{\mathrm{mod}}) \tag{10}$$

As each of the error criteria is likely to produce a different set of isotherm parameters, an overall optimum parameter set is difficult to identify directly. Hence, in order to try to make a meaningful comparison between the parameter sets, a procedure of normalizing and combining the error results was adopted, producing a so-called 'sum of the normalized errors' (SNE) for each parameter set for each isotherm. The calculation method for the SNE was as follows:

1) Select 1 isotherm and 1 error function and determine the isotherm parameters that minimize that error function for that isotherm to produce the isotherm parameter set for that error function;

2) Determine the values for all the other error functions for that isotherm parameter set;

3) Calculate all other parameter sets and all their associated error function values for that isotherm;

4) Select each error measure in turn and ratio the value of that error measure for a given parameter set to the largest value of that error from all the parameter sets for that isotherm; and

5) Sum all these normalized errors for each parameter set.

The parameter set thus providing the smallest normalized error sum can be considered to be optimal for that isotherm provided that:

•There is no bias in the data sampling, i.e. the experimental data are evenly distributed, providing an approximately equal number of points in each concentration range; and

•There is no bias in the type of error methods selected.

The 2-parameter isotherm models were fitted to the equilibrium biosorption data using both linear and nonlinear regression methods. The 3- and 4-parameter isotherm models were fitted to the equilibrium biosorption data using a nonlinear regression method only. The nonlinear regression routine of MATLAB 7.1 was used for the fitting. The results are shown in Tables 2a and 2b, respectively, and the modeled isotherms are plotted in Figures 6a–6d.

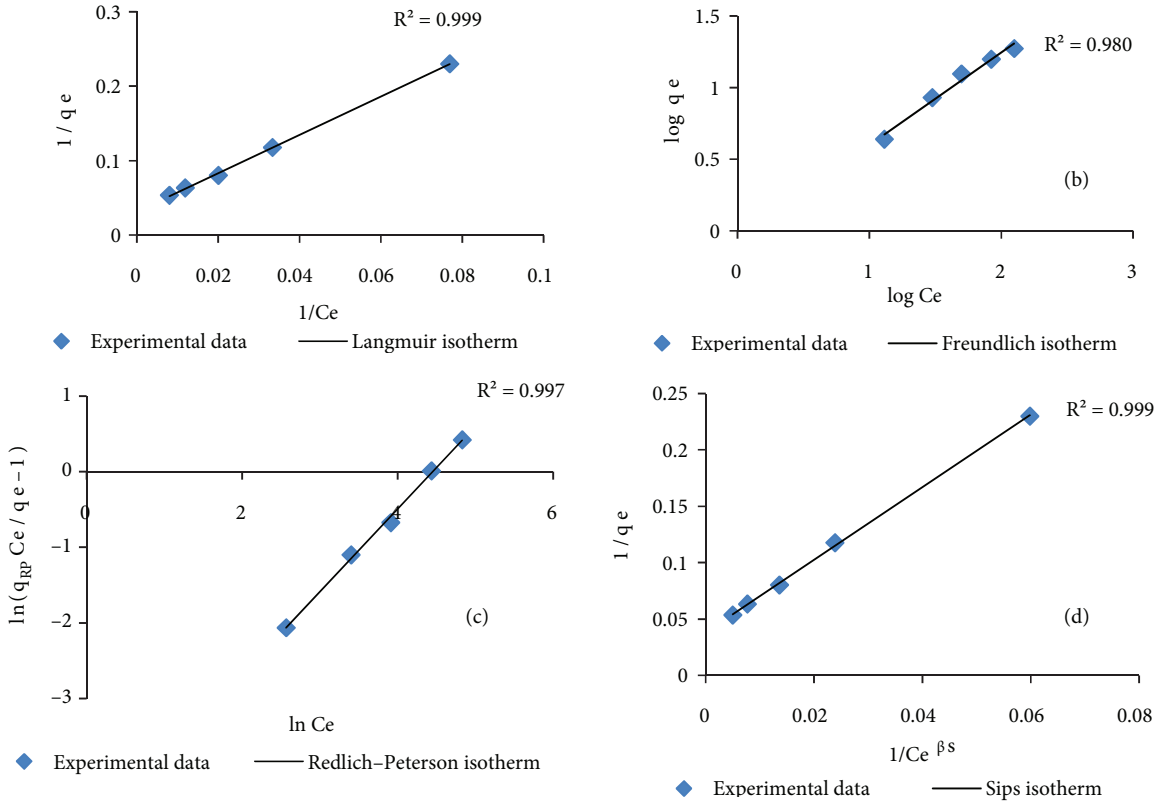

Figure 6. Linear regression fitting of adsorption isotherms to the batch equilibrium data of 2,4-DNP biosorption by chemically treated kola nut pod: (a) Langmuir isotherm, (b) Freundlich isotherm, (c) Redlich–Peterson isotherm, (d) Sips isotherm.

3.6.1. Langmuir isotherms

The Langmuir isotherm model [61] was used to describe observed biosorption phenomena. The Langmuir model is as given in Eq. (11):

$$q_e = \frac{Q_{\max} a C_e}{1 + a C_e}, \tag{11}$$

where $Q_{\max}$ and a are isotherm constants. The Langmuir constant ($Q_{\max}$) is a measure of the amount of naphthalene sorbed per unit weight of biosorbent, when saturation is attained. The Langmuir constant (a) is related to energy of adsorption (i.e. affinity of the binding sites), where $Q_{\max}$ and a can be determined from the linear plot of $1/q_e$ vs. $1/C_e$. The Langmuir equation is valid for monolayer sorption onto a surface with a finite number of identical sites that are homogeneously distributed over the sorbent surface [14]. The basic assumption of the Langmuir model is that sorption takes place at specific sites within the adsorbent. Theoretically, therefore,

a saturation value is reached beyond which no further sorption can take place. The sorption data were analyzed according to the linear form of the Langmuir isotherm. The linear plot of $1/q_e$ vs. $1/C_e$ is shown in Figure 6a and the linear isotherm constants a and $Q_{\max}$ and the error functions' values are presented in Table 2a. The isotherm was found to be linear over the whole concentration range studied with extremely high coefficients of determination (R^2) (Table 2a). Based on the R^2 value, the linear form of the Langmuir isotherm appears to produce a very good model for 2,4-DNP biosorption. The error function values also supported this assertion. The biosorption data were also analyzed according to the nonlinear form of the Langmuir isotherm as shown in Figure 7 and the Langmuir data from the other 5 error analysis methods are presented in Table 2b. The values of individual constants $Q_{\max}$ and a are very consistent across the range of error methods and are very close to those obtained by the linear error analysis approach. In all cases, all the error values for any of the parameter sets are lower than the same errors determined for the linear form of the isotherm. Considering the comparatively lower magnitudes of the error values together with the lower range of variation in the isotherm parameters suggests that the Langmuir isotherm does provide a particularly good model for the biosorption of 2,4-DNP onto chemically modified kola nut pod. Lastly, the HYBRID/MPSD/ARE parameter sets with lower SNE values produce the best overall fit for 2,4-DNP biosorption onto chemically modified kola nut pod.

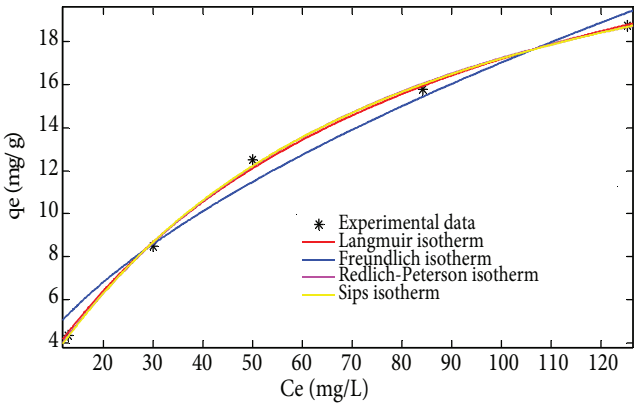

Figure 7. Nonlinear regression fitting of Langmuir, Freundlich, Redlich–Peterson, and Sips isotherms to the batch equilibrium data of 2,4-DNP biosorption by chemically treated kola nut pod.

Table 2. a) Isotherm constants with correlation coefficient and error analysis of 2-parameter isotherm models obtained through linear regression method for the 2,4-DNP and kola nut pod system.

Model	Langmuir	Freundlich	Redlich–Peterson	Sips
Parameters	Q_L32.26	K_F0.890	Q_{RP}0.377	Q_S26.32
	a_L0.012	$1/n$0.648	a_{RP}0.0077	a_S0.0118
			β_{RP}1.093	β_S1.098
Error functions				
R^2	**0.999**	0.980	0.997	**0.999**
ERRSQ	0.737	4.570	0.204	**0.189**
HYBRID	1.510	15.90	0.775	**0.762**
MPSD	15.10	39.90	8.80	**8.73**
ARE	0.907	6.360	0.310	**0.305**
EABS	0.713	0.288	**0.046**	0.137

The highest R^2 and lowest ERRSQ, HYBRID, MPSD, ARE, and EABS values are in bold.

Table 2. (b) Biosorption isotherm constants of 2- and 3-parameter isotherm models obtained through nonlinear regression analysis with error functions for the 2,4-DNP and kola nut pod system.

Isotherm models	Constants	ERRSQ	HYBRID	MPSD	ARE	EABS
Langmuir	Q_L	29.60	30.10	30.10	30.10	29.90
	a_L	0.014	0.013	0.013	0.013	0.014
	ERRSQ	**0.230**	0.247	0.247	0.247	0.239
	HYBRID	0.770	**0.704**	**0.704**	**0.704**	0.711
	MPSD	8.740	**8.350**	**8.350**	**8.350**	8.390
	ARE	0.463	**0.423**	**0.423**	**0.423**	0.427
	EABS	0.097	**0.021**	**0.021**	**0.021**	0.035
	SNE	4.93	**3.99**	**3.99**	**3.99**	4.13
Freundlich	K_f	1.244	1.031	1.031	1.031	1.035
	$1/n$	0.5	0.611	0.611	0.611	0.610
	ERRSQ	**2.505**	3.020	3.020	3.020	3.000
	HYBRID	11.20	**8.960**	**8.960**	**8.960**	**8.960**
	MPSD	33.30	**29.80**	**29.80**	**29.80**	**29.80**
	ARE	6.710	**5.380**	**5.380**	**5.380**	**5.380**
	EABS	0.284	0.269	0.269	0.269	**0.247**
	SNE	4.83	4.43	4.43	4.43	**4.36**
Redlich–Peterson	Q_{RP}	0.376	0.371	0.371	0.371	0.369
	a_{RP}	0.0067	0.0059	0.0059	0.0059	0.0066
	β_{RP}	1.124	1.146	1.146	1.146	1.119
	ERRSQ	**0.176**	0.178	0.178	0.178	0.207
	HYBRID	0.694	**0.681**	**0.681**	**0.681**	0.818
	MPSD	8.330	**8.250**	**8.250**	**8.250**	9.040
	ARE	0.278	**0.272**	**0.272**	**0.272**	0.327
	EABS	0.021	**0.013**	**0.013**	**0.014**	0.209
	SNE	3.57	**3.50**	**3.50**	**3.50**	5.00
Sips	Q_S	26.88	27.09	27.09	27.09	28.25
	a_S	0.0116	0.0117	0.0117	0.0117	0.0113
	β_S	1.093	1.086	1.086	1.086	1.070
	ERRSQ	**0.162**	**0.162**	**0.162**	**0.162**	0.231
	HYBRID	0.675	**0.672**	**0.672**	**0.672**	0.957
	MPSD	8.220	**8.200**	**8.200**	**8.200**	9.780
	ARE	0.270	**0.269**	**0.269**	**0.269**	0.383
	EABS	0.030	**0.014**	**0.014**	**0.014**	0.125
	SNE	3.19	**3.05**	**3.05**	**3.05**	5.00

The lowest ERRSQ, HYBRID, MPSD, ARE, EABS, and SNE values for each isotherm model are in bold.

It can be explained apparently that when $a > 0$, the sorption system is favorable [62]. In this study, a was found to be 0.012 L/mg with linear regression analysis and 0.013 L/mg with nonlinear regression analysis. The maximum monolayer biosorption capacity ($Q_{\max}$) was obtained to be 32.26 mg/g (linear regression) and 30.10 mg/g (nonlinear regression). Potgieter et al. [37] obtained 0.564 mg/g and 0.145 mg/g as the maximum monolayer adsorption capacity of South African fly ash for the adsorption of 2-nitrophenol and 4-nitrophenol, respectively. Varank et al. [1], Ofomaja [63], and Li et al. [64] correspondingly reported values of 15.19 mg/g and 12.70 mg/g, 21.28 mg/g, and 1.98 mg/g as the maximum adsorption capacity of bentonite and zeolite, mansonia sawdust, and chitosan for the adsorption of 4-nitrophenol, respectively.

The shape of the Langmuir isotherm can be used to predict whether a sorption system is favorable or unfavorable in a batch adsorption process. The essential characteristics of Langmuir isotherms can be described by a separation factor [65–67], which is defined in Eq. (12) as:

$$R_L = \frac{1}{(1 + aC_o)}. \tag{12}$$

The separation factor (R_L) indicates the isotherm shape as follows: $R_L < 1$ unfavorable, $R_L > 1$ unfavorable, $R_L = 1$ linear, $0 < R_L < 1$ favorable, and $R_L = 0$ irreversible. The separation factor obtained at different initial 2,4-DNP concentrations is presented in Table 3. The R_L ranges from 0.1429 to 0.4545 (using the constant a value obtained from the linear plot) and this indicate a favorable biosorption process.

Table 3. Separation factor (R_L) obtained for the biosorption of 2,4-DNP by chemically treated kola nut pod.

Initial concentration (mg/L)	Separation factor (R_L)
100	0.4545
200	0.2941
300	0.2174
400	0.1724
500	0.1429

3.6.2. Freundlich isotherm

The Freundlich isotherm model [68] is given in Eq. (13):

$$q_e = K_f C_e^{1/n}, \tag{13}$$

where K_f and n are Freundlich constants. K_f is roughly an indicator of the adsorption capacity (mg/g) and n is the adsorption intensity. The Freundlich isotherm is used for nonideal adsorption on heterogeneous surface energy systems [44]. It suggests that binding sites are not equivalent and/or independent. McKay et al. [69] and Annadurai et al. [66] stated that the magnitude of the exponent $^1/_n$ gives an indication of the favorability and capacity of the adsorbent/adsorbate system. Values of $n > 1$ represent favorable adsorption conditions according to Treybal [70]. In most cases, an exponent between $1 < n < 10$ shows beneficial adsorption.

K_f and $1/n$ were determined from the linear plot of $\log q_e$ vs. $\log C_e$ as shown in Figure 6b. The evaluated constants are given in Table 2a. Examination of the plot suggests that the linear Freundlich isotherm is a good model for the sorption of 2,4-DNP. Table 2a shows the linear Freundlich sorption isotherm constants, coefficients of determination (R^2), and error function values. Based on the R^2 value, the linear form of the Freundlich isotherm appears to produce a reasonable model for 2,4-DNP sorption. However, the comparative magnitude of the error function values does not support this assertion. The Freundlich isotherm constants determined by nonlinear regression are shown in Figure 7 and the parameter set provided by the error functions is presented in Table 2b. The results demonstrate that the values of constants $1/n$ and K_f obtained by nonlinear regression are remarkably consistent. The minimum error occurs for the constants determined using the EABS and the set parameters are quite similar to those obtained by linearization. In this study, K_f and $1/n$ were found to be 0.891 mg/g(L/mg)$^{1/n}$ and 0.648 from the linear plot and 1.035 mg/g(L/mg)$^{1/n}$ and 0.610 from the nonlinear plot, respectively. Thus, the n value is 1.54 (linear value) and 1.64 (nonlinear value)

(greater than unity). From other studies in the literature, the values of K_f:n obtained for the adsorption of 4-nitrophenol onto other adsorbents are 1.89:2.33 for zeolite [1], 0.160:1.17 for bentonite [1], 0.063:1.00 for South African fly ash [42], and 4.16:2.08 for palm oil fuel ash [47]. Potgieter et al. [42] also reported that the values of K_f and n for the adsorption of 2-nitrophenol onto South African fly ash were 0.054 and 1.04, respectively.

3.6.3. Redlich–Peterson isotherm

The Redlich–Peterson isotherm equation contains 3 parameters and incorporates the features of the Langmuir and Freundlich isotherms [71]. This isotherm equation is as given in Eq. (14):

$$q_e = \frac{Q_{RP} C_e}{1 + a_{RP} C_e^{\beta_{RP}}}, \tag{14}$$

where Q_{RP} is the maximum biosorption capacity, a_{RP} is the Redlich–Peterson model constant (L/mg), and β_{RP} is the Redlich–Peterson model exponent. The exponent β_{RP} lies between 0 and 1. There are 2 limiting behaviors: the Langmuir form for $\beta_R = 1$ and the Henry's law form for $\beta_{RP} = 0$ [72]. At low adsorbate concentrations, the Redlich–Peterson isotherms approximate Henry's law, and at high adsorbate concentrations, the behavior approaches that of the Freundlich isotherm [73]. Although linear analysis is not possible for a 3-parameter isotherm, a trial-and-error procedure has previously been applied to a pseudo-linear form of the Redlich–Peterson isotherm to obtain values for the isotherm constants [74]. The method is based on the following equation:

$$\ln(Q_{RP}\frac{C_e}{q_e} - 1) = \beta_{RP} \ln C_e + \ln(a_{RP}). \tag{15}$$

The method involves varying the isotherm parameter, Q_{RP}, to obtain the maximum value of the correlation coefficient for the regression of $\ln(Q_{RP}C_e/q_e - 1)$ against $\ln(C_e)$. Examination of the plot (Figure 6c) shows that the Redlich–Peterson isotherm accurately describes the sorption behavior of 2,4-DNP over the concentration ranges studied. The Redlich–Peterson isotherm constants and the coefficients of determination are presented in Table 2a. Since the method used to derive the isotherm parameters maximizes the linear correlation coefficient, it is not surprising that the Redlich–Peterson isotherms exhibit extremely high R^2 values, indicating a considerably better fit compared to the Freundlich isotherm. The application of the isotherm to the equilibrium biosorption data using a nonlinear regression method is shown in Figure 7, and the estimated isotherm constants from the nonlinear error analyses are presented in Table 2b. Similar to the nonlinear Freundlich analysis, the Redlich–Peterson isotherm constants are very consistent across the range of error methods and the actual parameter values derived by nonlinear regression are very close to those obtained using the linear analysis. The lowest SNE was obtained using the HYBRID/MPSD/ARE parameter sets.

3.6.4. Sips Isotherm Model

The Sips isotherm model [75] is also a 3-parameter model. It is a combined form of Langmuir and Freundlich expressions deduced for predicting heterogeneous adsorption systems and circumventing the limitation of the rising adsorbate concentration associated with Freundlich isotherm model. The isotherm model is represented as in Eq. (16):

$$q_e = \frac{Q_S a_S C_e^{\beta_S}}{1 + a_S C_e^{\beta_S}}. \tag{16}$$

At low adsorbate concentrations, it reduces to a Freundlich isotherm, while at high concentrations, it predicts a monolayer adsorption capacity characteristic of the Langmuir isotherm [76]. The pseudo-linear form of Eq. (17) can be written as:

$$\frac{1}{q_e} = \frac{1}{a_S Q_S} * \frac{1}{C_e^{\beta_S}} + \frac{1}{Q_S}. \tag{17}$$

The method involves varying the isotherm parameter β_S to obtain the maximum value of the correlation coefficient for the regression of $1/q_e$ against $1/C_e^{\beta_S}$. Examination of the plot (Figure 6d) shows that the Sips isotherm accurately describes the sorption behavior of 2,4-DNP over the concentration ranges studied. The Sips isotherm constants and the coefficients of determination are presented in Table 2a. Similar to the Redlich–Peterson isotherm, based on the R^2 value, the pseudo-linear form of the Sips isotherm appears to produce a very good model for 2,4-DNP sorption and the comparative lower magnitude of the error function values supports this assertion. The application of the isotherm to the equilibrium biosorption data using a nonlinear regression method is shown in Figure 7, and the estimated isotherm constants from the 5 nonlinear error analyses are presented in Table 2b. Similar to the nonlinear Redlich–Peterson analysis, Table 2b shows that the Sips isotherm constants are very consistent across the range of error methods and the actual parameter values derived by nonlinear regression are very close to those obtained using the linear analysis. The lowest SNE was obtained using the HYBRID/MPSD/ARE parameter sets. The model exponent (β_S) value is marginally greater than or equal to unity, indicating that the biosorption of 2,4-DNP by chemically modified kola nut pod is more of Langmuir form rather than of Freundlich.

3.6.5. Error analysis – comparison of isotherm models

Tables 2a and 2b show the linear and nonlinear parameter set values for 2 of 2-parameter and 2 of 3-parameter isotherm models. As seen from Table 2a, the highest linear regression coefficient of determination (R^2) was obtained for the experimental data using the Langmuir isotherm, closely followed by the Redlich–Peterson isotherm. According to Ho et al. [19], selection of the linear isotherm transformation with the highest linear regression R^2 does not appear to be the most appropriate method to choose a model for sorption equilibria. Several other error functions can be used for model selection. Therefore, based on the 5 measured error functions, the Langmuir isotherm produced the better fit of the 2-parameter isotherm models examined, having the lowest error values. Furthermore, based on any of the error functions, better fits can be obtained for most 2-parameter isotherms by using nonlinear regression [19]. For the 2-parameter isotherms examined using nonlinear regression analysis, the HYBRID/MPSD/ARE error functions produced the parameter set providing the lowest SNE in 1 of the 2 isotherms, and the EABS produced the parameter set for the second isotherm. In addition, the error values determined by nonlinear regression are lower than those for the linear isotherm parameters. This indicates that the nonlinear equation analysis method may be a suitable approach to use for 2-parameter isotherms. Nevertheless, the linear parameters provided reasonably close estimates to the optimized nonlinear solutions for 2,4-DNP and kola nut pod systems and the same trend of fitting as that of nonlinear regression was produced by the linear regression analysis: Langmuir > Freundlich. Therefore, both linear and nonlinear regression methods may be used for the analysis of 2-parameter adsorption isotherms.

For the 3-parameter isotherms, the HYBRID/MPSD/ARE error functions produced the parameter sets providing the lowest SNE in the 2 isotherms examined, with the ERRSQ error function giving the second lowest value in each case and therefore providing the next best-fitting isotherm constants. Similarly, like the 2-parameter isotherms, the error values determined by nonlinear regression are lower than those for the linear

isotherm parameters. This affirms the fact that the nonlinear equation analysis method is a suitable approach to use for the 3-parameter isotherms, although the linear parameters provided reasonably close estimates to the optimized nonlinear solutions for 2,4-DNP and kola nut pod. Based on the lowest SNE value, among the 3-parameter isotherm models, the order of best fit is as follows: Sips > Redlich–Peterson. In this study, the 3-parameter isotherms were found to provide a better match to the experimental data than the 2-parameter isotherms. This is in agreement with the observation of Ho et al. [19] in their study of divalent metal ions sorption onto peat.

The error functions HYBRID and MPSD could be accepted as the most indicative, adequate, and essentially meaningful when determining the best-fitting isotherm model, as the number of isotherm parameters is accounted for only by them [60,77]. This assertion is supported by the data in Table 2b, as the 3-parameter isotherm models were characterized with higher extent of suitability to the experimental data due to lower error values. A similar observation was reported in a previous study [19]. Generally, among the 4 isotherm models applied to the equilibrium biosorption experimental data, HYBRID/MPSD/ARE error functions provided 3 of the lowest SNE values, and the Sips isotherm equation employing the parameter set derived using the HYBRID/MPSD/ARE errors provided the overall best model for the experimental system. Therefore, considering the lower SNE values obtained for the 4 isotherm models, the order of prediction precision is determined as follows: Sips > Redlich–Peterson > Langmuir > Freundlich.

3.7. Kinetic modeling of biosorption

Mass transfers occur within the boundary layer around the biosorbent and proceed in the liquid-filled pores or along the walls of the pores of biosorbent, which are called external and internal mass transfers, respectively. Typical kinetic models normally consider both the external and internal mass transfers. Examples of these models are film-pore diffusion, film-surface diffusion, pore diffusion, surface diffusion, and combined pore and surface diffusion models. These models involve complicated mathematical computations in order to obtain the related diffusion coefficients of the models. Furthermore, the mass transfers of adsorption or biosorption often involve many controlling mechanisms, of which the individual contribution may not be clearly recognized, at the same time during the course to approach adsorption equilibria [78]. Therefore, for the simplicity and practical use of engineering applications, global kinetic expressions such as the Lagergren pseudo-first-order [79], pseudo-second-order [80], Elovich [81], power function [82], and intraparticle diffusion [83] rate equations were adopted and applied to the biosorption data in order to analyze the rate of biosorption and possible adsorption mechanism of naphthalene onto modified spent tea leaves.

3.7.1. Pseudo-first-order kinetic model

The Lagergren pseudo-first-order kinetic model equation [79,84] is represented in an integral form as given in Eq. (18):

$$\ln(q_e - q_t) = \ln q_e - k_1 t, \tag{18}$$

where q_e is the theoretical equilibrium biosorption capacity (mg/g) and k_1 is the biosorption rate constant ($\min^{-1}$). The plots of $\ln(q_e - q_t)$ versus t give a straight line (Figure 8). The values of the rate constants k_1 and theoretical equilibrium biosorption capacities q_e(theoretical) at different concentrations and temperatures were calculated from the slopes and intercepts of the linear plots. The respective values are given in Table 4. It is required that the theoretically calculated equilibrium biosorption capacity, q_e (theor.), be in accordance with the experimental biosorption capacity, q_e (exp.), values [85]. From Table 4, it was found that the correlation

coefficients (R^2) are relatively high and there is good agreement between q_e (theoretical) and q_e (experimental). This suggests that the biosorption of 2,4-DNP by chemically treated kola nut pod follows first-order reaction kinetics. It can also be seen from Table 4 that the biosorption rate constant (k_1) generally remained constant with an increase in initial 2,4-DNP concentration and decreased with an increase in temperature.

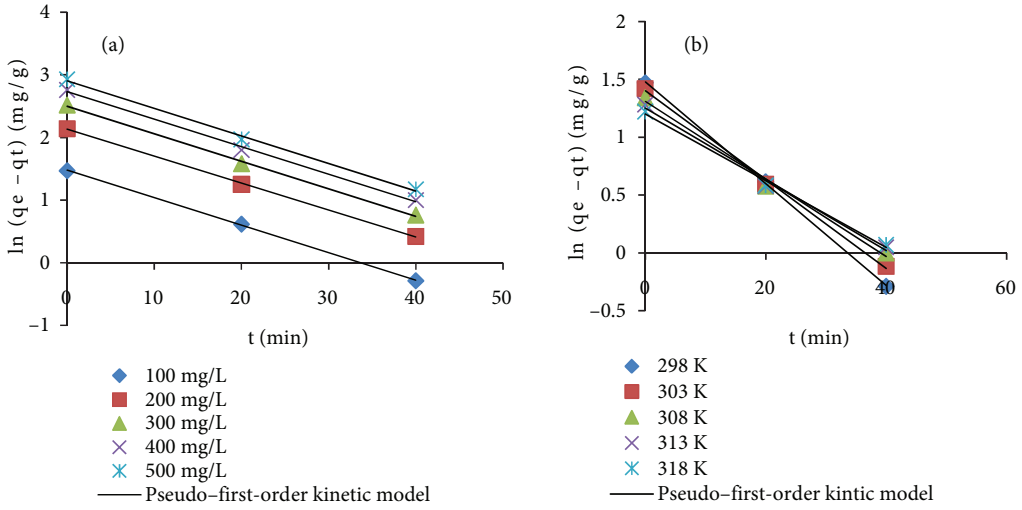

Figure 8. Pseudo-first-order kinetic model fitted to the batch kinetic data of 2,4-DNP biosorption by chemically treated kola nut pod at different (a) initial 2,4-DNP concentrations and (b) temperatures.

3.7.2. Pseudo-second-order kinetic model

The pseudo-second-order kinetic model, which is based on the assumption that chemisorption is the rate-determining step, can be expressed as:

$$\frac{t}{q_t} = \frac{1}{k_2 q_e^2} + \frac{t}{q_e}, \tag{19}$$

where k_2 is the rate constant of second-order biosorption (g mg^{-1} min^{-1}) and q_e is the theoretical equilibrium biosorption capacity (mg/g). The initial biosorption rate, h (mg g^{-1} min^{-1}), is represented in Eq. (20) [86]:

$$h = k_2 q_e^2. \tag{20}$$

The plots of t/q_t versus t give a straight line (Figure 9). Values of k_2 and q_e were calculated from the linear plots of t/q_t vs. t (Figure 9) for different initial concentrations and temperatures. The respective constant values are given in Table 4. The high correlation coefficients (R^2) of the pseudo-second-order (Table 4) suggest the applicability of the pseudo-second-order kinetic model to fit the experimental data. It is also expected that the theoretically calculated equilibrium biosorption capacity, q_e (theor.), be in accordance with the experimental adsorption capacity, q_e (exp.), values. It could be seen from Table 4 that the correlation coefficients (R^2) are high but relatively lower than the results obtained for pseudo-first-order kinetics, and there is not very good agreement between q_e (theoretical) and q_e (experimental). Therefore, this suggests that the biosorption of 2,4-DNP by chemically treated kola nut pods does not follow a pseudo-second-order type of reaction kinetics.

Table 4. Pseudo-first-order, pseudo-second-order, Elovich, power function, intraparticle, and liquid film diffusion kinetic parameters and correlation coefficients obtained for the biosorption of 2,4-DNP by chemically treated kola nut pod.

Kinetic model		Initial concentration (mg/L)					Temperature (K)				
		100	200	300	400	500	298	303	308	313	318
Pseudo-first-order	k_1^a	0.044	0.044	0.044	0.044	0.044	0.044	0.038	0.033	0.030	0.028
	q_e^b(theor.)	4.380	8.410	12.18	15.38	18.23	4.380	4.060	3.700	3.490	3.320
	q_e(exp.)	4.350	8.500	12.49	15.79	18.74	4.350	4.150	3.850	3.600	3.400
	R^2	0.999	0.999	0.998	0.997	0.997	0.999	0.998	0.993	0.993	0.996
Pseudo -second-order											
	k_2^c	0.030	0.017	0.013	0.013	0.012	0.030	0.025	0.021	0.019	0.018
	q_e(theor.)	4.720	9.090	13.33	16.67	19.61	4.720	4.480	4.260	4.030	3.880
	h^d	0.668	1.405	2.310	3.613	4.615	0.668	0.502	0.381	0.309	0.271
	R^2	0.974	0.983	0.986	0.991	0.992	0.974	0.968	0.955	0.939	0.922
Elovich											
	α^e	0.540	1.730	1.940	2.510	2.950	0.540	0.450	0.350	0.280	0.230
	β^f	0.820	0.500	0.310	0.250	0.210	0.820	0.820	0.820	0.820	0.820
	R^2	0.908	0.915	0.913	0.914	0.914	0.908	0.915	0.911	0.907	0.906
Power function											
	a	0.900	2.420	3.060	3.930	4.660	0.900	0.780	0.610	0.470	0.370
	b	0.359	0.285	0.320	0.316	0.316	0.359	0.380	0.417	0.461	0.505
	R^2	0.911	0.933	0.923	0.924	0.924	0.911	0.929	0.934	0.935	0.935
Intraparticle diffusion											
	K_p	0.341	0.564	0.904	1.132	1.347	0.341	0.343	0.345	0.349	0.351
	C	1.270	3.373	4.314	5.554	6.553	1.270	1.032	0.701	0.418	0.191
	R^2	0.840	0.861	0.849	0.851	0.851	0.840	0.858	0.864	0.865	0.864
Liquid film diffusion											
	D	0.044	0.044	0.044	0.044	0.044	0.044	0.038	0.033	0.030	0.028
	R^2	0.999	0.999	0.998	0.997	0.997	0.999	0.998	0.993	0.993	0.996

^{a} = min^{-1}, ^{b} = mg/g, ^{c} = g/(mg min), ^{d} = mg g^{-1} min^{-1}, ^{e} = mg/(g min), ^{f} = g/mg.

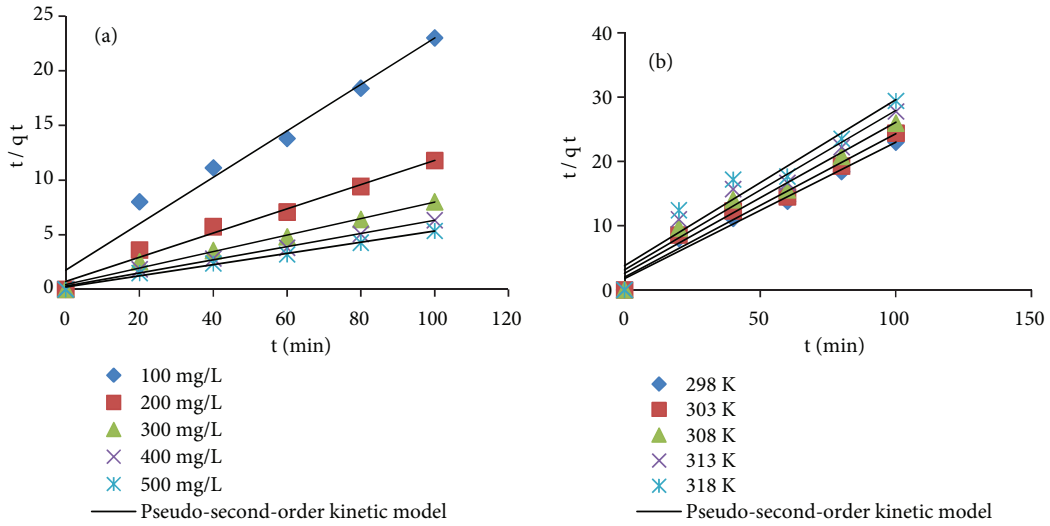

Figure 9. Pseudo-second-order kinetic model fitted to the batch kinetic data of 2,4-DNP biosorption by chemically treated kola nut pod at different (a) initial 2,4-DNP concentrations and (b) temperatures.

Moreover, it was observed that the second-order rate constant k_2 generally decreased with increase in initial 2,4-DNP concentration. This is due to the lower competition for the surface active sites at lower concentrations, but at higher concentrations the competition for the surface active sites will be high and consequently lower biosorption rates will be obtained. Furthermore, it can be seen from Table 4 that second-order rate constant, k_2, decreased as the temperature increased, indicating the exothermic nature of 2,4-DNP biosorption by chemically treated kola nut pod surface. Again, as evident from Table 4, the initial adsorption rate, h, increased with increase in initial 2,4-DNP concentration and decreased with increase in temperature, suggesting that biosorption of 2,4-DNP by chemically treated kola nut pod was favorable at higher concentrations and lower temperatures. The increase in initial biosorption rate with increase in 2,4-DNP concentration may be due to the increased concentration gradient, which acts as an increased driving force to overcome the resistances to mass transfer of 2,4-DNP between the aqueous phase and the solid phase [41,87]. Meanwhile the decrease in initial biosorption rate with increased temperature could probably be due to decreased kinetic energy gained by the 2,4-DNP molecules, thereby resulting in a decreased temperature gradient that acted as a driving force for the molecular transfer of 2,4-DNP from the aqueous system to the biosorbent (solid system).

3.7.3. Elovich kinetic model

The Elovich equation [53,81], which is used to express the mechanism of adsorption, can generally be expressed as presented in Eq. (21):

$$\frac{dq_t}{dt} = \alpha \exp(-\beta q_t). \tag{21}$$

To simplify the Elovich equation, Chien and Clayton [88] assumed $\alpha\beta t >> 1$, and by applying the boundary conditions $q_t = 0$ at $t = 0$ and $q_t = q_t$ at $t = t$, Eq. (21) becomes [89]:

$$q_t = \frac{1}{\beta}\ln(\alpha\beta) + \frac{1}{\beta}\ln t, \tag{22}$$

where α is the initial biosorption rate (mg g^{-1} min^{-1}) and β is the desorption constant (g/mg).

The Elovich equation has been shown to be useful in describing chemisorption on highly heterogeneous adsorbents. The values of α and β were calculated from the plots of q_t vs. $\ln t$ (Figure 10). The respective constant values are given in Table 4. The calculated values of α and β showed a general trend of changes with an increase in the initial 2,4-DNP concentration and temperature, respectively. The initial biosorption rate (α) increased with increase in initial 2,4-DNP concentration and decreased with increase in temperature. This suggests that the biosorption process was chemisorption corresponding to the heterogeneous nature of the active sites while the desorption constant (β) decreased with increase in initial concentration and did not vary with increase in solution temperature. Thus, $1/\beta$ (which is apparently indicative of the number of sites available for biosorption) showed a distinct increase with an increase in concentration and remained constant with increase in temperature, again reinforcing the occurrence of chemisorption.

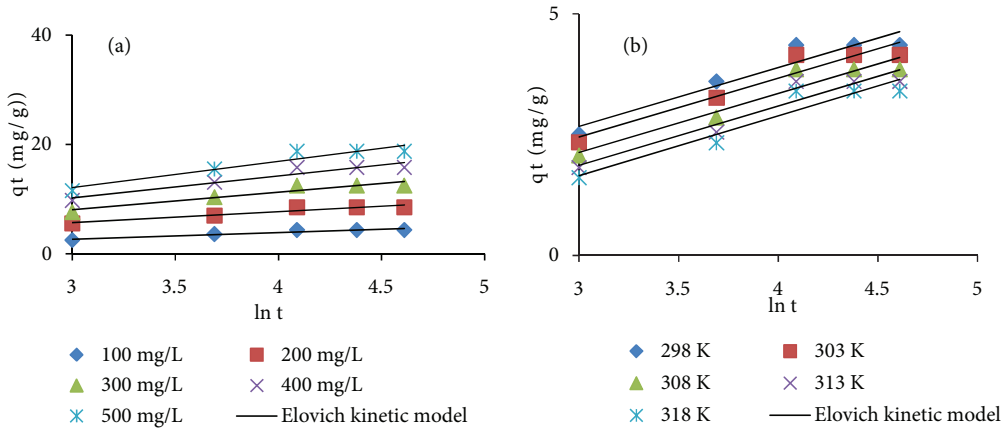

Figure 10. Elovich kinetic model fitted to the batch kinetic data of 2,4-DNP biosorption by chemically treated kola nut pod at different (a) initial 2,4-DNP concentrations and (b) temperatures.

3.7.4. Power function model

The power function kinetic equation develops a relation between contaminant uptake onto the adsorbent and time t, and the equation was given by Goswami and Ghosh [82]:

$$\log q_t = \log a + b \log t. \tag{23}$$

A linear plot (Figure 11) between log q vs. log t gives the constants of power functions a and b. The constants a and b represent the initial rate and rate constant of the reaction (Table 4). The initial rate constant a increases with increase in initial 2,4-DNP concentration and decreases with increase in solution temperature, while the rate constant b generally decreases with increase in initial 2,4-DNP and increases with increase in solution temperature.

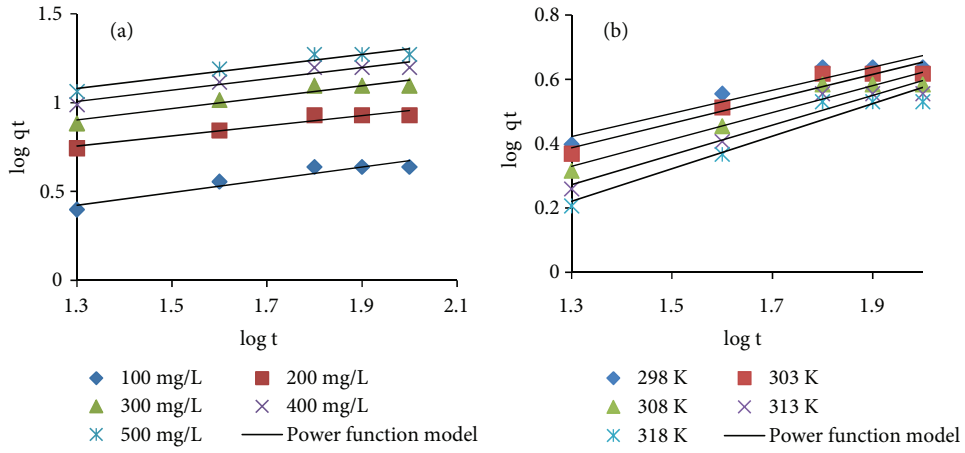

Figure 11. Power function kinetic model fitted to the batch kinetic data of 2,4-DNP biosorption by chemically treated kola nut pod at different (a) initial 2,4-DNP concentrations and (b) temperatures.

3.7.5. Biosorption mechanisms

A detailed understanding of adsorption or biosorption mechanisms facilitates a determination of the rate-limiting step. This information can then be used to optimize the design of adsorbent/biosorbents and adsorption/biosorption conditions. The overall rate of biosorption can be described by the following 3 steps [90]: 1) film or surface diffusion where the sorbate is transported from the bulk solution to the external surface of sorbent; 2) intraparticle or pore diffusion, where sorbate molecules move into the interior of sorbent particles; and 3) adsorption on the interior sites of the sorbent. Since the adsorption/biosorption step is very rapid, it is assumed that it does not influence the overall kinetics. The overall rate of biosorption process, therefore, will be controlled by either surface diffusion or intraparticle diffusion. The Weber–Morris intraparticle diffusion model has often been used to determine if intraparticle diffusion is the rate-limiting step [81,82].

3.7.5.1. Intraparticle diffusion model

The intraparticle diffusion kinetic model [83] can be written as presented in Eq. (24):

$$q_t = K_p t^{0.5} + C, \tag{24}$$

where K_p is the intraparticle diffusion rate constant (mg g^{-1} min$^{-1/2}$) and C is the intercept.

The intercept of the plot reflects the boundary layer effect. The larger the intercept, the greater is the contribution of the surface sorption in the rate-controlling step. According to this model, a plot of q_t vs. $t^{0.5}$ should be linear if intraparticle diffusion is involved in the adsorption process, and if the plot passes through the origin, then intraparticle diffusion is the sole rate-limiting step [91]. It has also been suggested that in instances when q_t vs. $t^{0.5}$ is multilinear 2 or more steps govern the adsorption/biosorption process [82,92]. In fact, the linear plots at each concentration and temperature (Figure 12) did not pass through the origin and, given the multilinearity of this plot for biosorption of 2,4-DNP onto chemically treated kola nut pod, this suggests that biosorption occurred in 3 phases (Figure 12). The initial steeper section represents surface or film diffusion, the second linear section represents a gradual biosorption stage where intraparticle or pore diffusion is rate-limiting, and the third section is a final equilibrium stage where intraparticle diffusion starts to slow down due to the extremely low adsorbate concentrations in the solution [93]. As the plot did not pass through the origin, intraparticle diffusion was not the only rate-limiting step. Thus, there were 3 processes controlling the biosorption rate, but only 1 process was rate-limiting in any particular time range. The intraparticle diffusion rate constant K_p was calculated from the slope of the second linear section and the values are presented in Table 4. The K_p values increased with the increase in initial 2,4-DNP concentration and solution temperature. The value of intercept C provides information related to the thickness of the boundary layer [94]. Larger intercepts suggest that surface diffusion has a larger role as the rate-limiting step. The intercept values increased with increase in initial 2,4-DNP concentration and decreased with increasing temperature.

3.7.5.2. Liquid film diffusion model

The liquid film diffusion model [95] was also employed to investigate whether the transport of the sorbate molecules from the liquid phase up to the solid phase boundary plays a major role in the biosorption, as shown in Eq. (25):

$$-\ln(1 - F) = Dt, \tag{25}$$

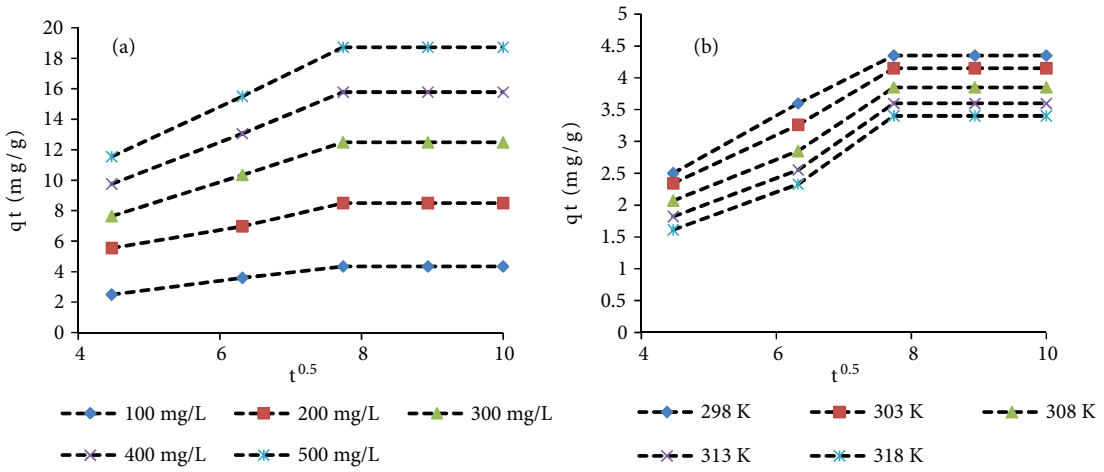

Figure 12. Intraparticle diffusion kinetic model fitted to the batch kinetic data of 2,4-DNP biosorption by chemically treated kola nut pod at different (a) initial 2,4-DNP concentrations and (b) temperatures.

where F is the fractional attainment of equilibrium $F = q_t/q_e$, and D is the liquid diffusion constant. A linear plot of –ln (1 – F) versus t with zero intercept would suggest that the kinetics of the biosorption process are controlled by diffusion through the liquid surrounding the solid sorbent. In this study, the linear regression line did not pass through the origin but was closer to the origin (Figure 13), and the high regression values ($R^2 > 0.99$) at different initial concentrations and temperatures show the relevance of film diffusion as a rate-determining factor in the biosorption process. The liquid film diffusion constant D did not vary with increase in initial 2,4-DNP concentrations; however, it decreased with increase in solution temperature (Table 4).

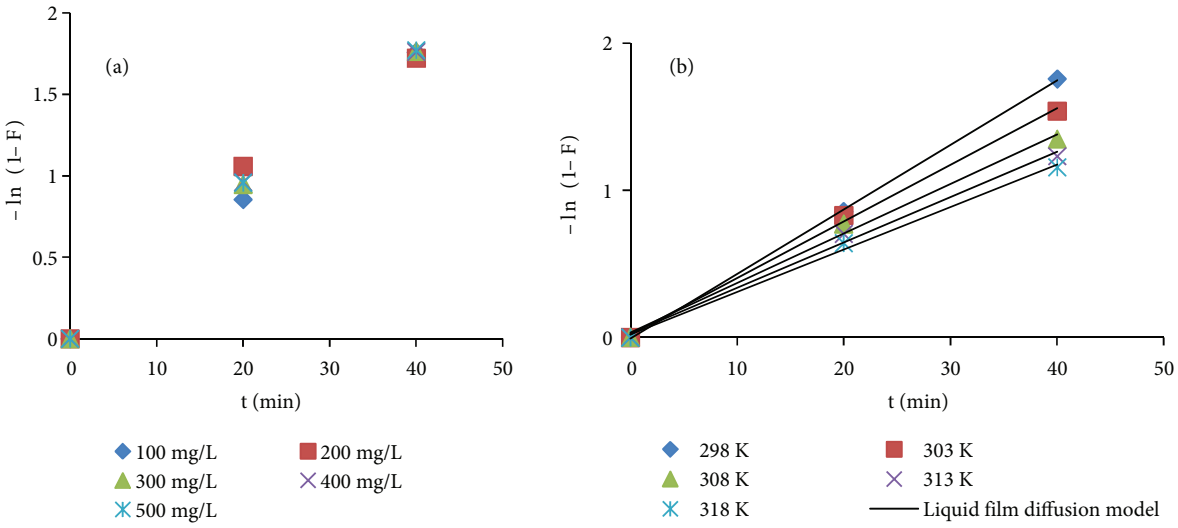

Figure 13. Liquid film diffusion kinetic model fitted to the batch kinetic data of 2,4-DNP biosorption by chemically treated kola nut pod at different (a) initial 2,4-DNP concentrations and (b) temperatures.

Generally, all the tested biosorption kinetic models fit well to the biosorption kinetic data with high correlation coefficients at different initial 2,4-DNP concentrations and solution temperatures; however, the pseudo-first-order kinetic model gave the best fit with higher correlation coefficients ($R^2 > 0.99$) to describe

the biosorption behavior of 2,4-DNP by chemically treated kola nut pod. Similar observations were reported for the adsorption of 4-nitrophenol onto magnesium-aluminum mixed oxide [25].

3.8. Thermodynamic modeling

In order to study the feasibility of the biosorption process, thermodynamic parameters such as standard Gibb's free energy change (ΔG^o), standard enthalpy change (ΔH^o), and standard entropy change (ΔS^o) can be estimated from Eq. (26) [36]:

$$\ln K_D = \frac{\Delta S^o}{R} - \frac{\Delta H^o}{RT}, \tag{26}$$

where K_D is the distribution coefficient of the biosorbent and is equal to q_e/C_e, T (K) is the absolute solution temperature, and R is the universal gas constant (8.314 J/mol K). ΔH^o can be calculated from the slope and ΔS^o can be calculated from the intercept of the Van't Hoff plot of $\ln K_D$ vs. $1/T$ shown in Figure 14a. ΔG^o can then be calculated using the following equation:

$$\Delta G^o = \Delta H^o - T\Delta S^o. \tag{27}$$

From the pseudo-first-order rate constant k_1 (Table 4), the activation energy E_a for the biosorption of 2,4-DNP by chemically treated kola nut pod surface was determined using the Arrhenius equation (Eq. 28):

$$\ln k_1 = \ln A - \frac{E_a}{RT}, \tag{28}$$

where k_1 is the biosorption rate constant, A is the Arrhenius constant, E_a is the activation energy (kJ mol^{-1}), R is the gas constant (8.314 J mol^{-1} K^{-1}), and T is the temperature (K). By plotting $\ln k_1$ vs. $1/T$, E_a was obtained from the slope of the linear plot (Figure 14b) and is presented in Table 5.

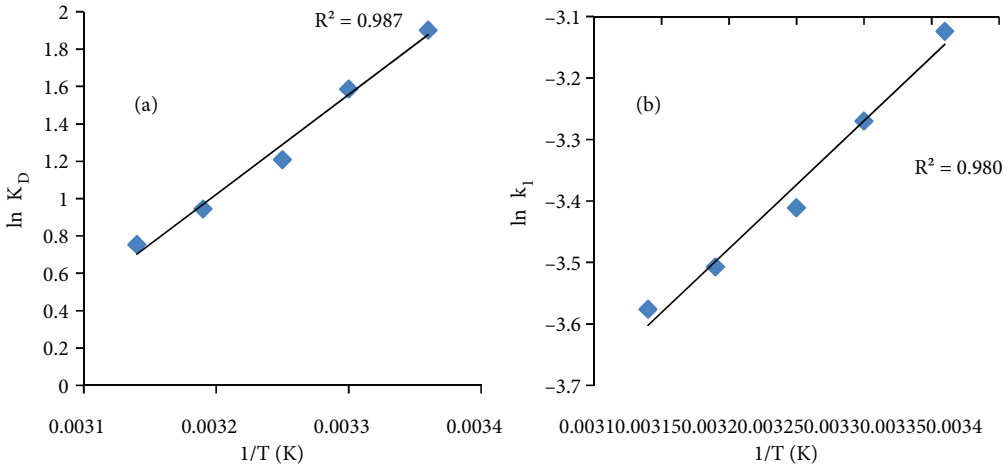

Figure 14. Plots to estimate the thermodynamic properties of 2,4-DNP biosorption by chemically treated kola nut pod: (a) plot of ln K_D versus 1/T to estimate standard enthalpy (ΔH°) and standard entropy (ΔS°), and (b) plot of ln k_1 versus 1/T to estimate activation energy from Arrhenius equation fitted to the batch kinetic data at different temperatures.

Table 5. Thermodynamic parameters for the biosorption of 2,4-DNP by chemically treated kola nut pod.

Temperature (K)	ΔG^o(kJ/mol)	ΔH^o(kJ/mol)	ΔS^o(kJ/mol)	E_a(kJ/mol)
298	–4.74	–44.37	–0.133	–17.26
303	–4.07			
308	–3.41			
313	–2.74			
318	–2.08			

From Table 5, it is clear that the reaction is spontaneous in nature as ΔG^o values are negative at all the temperatures studied. Increase in the negative value of ΔG^o with decrease in temperature suggests that a lower temperature makes the biosorption easier. Generally, ΔG^o values range from 0 to –20 kJ/mol for physical adsorption and –80 to –400 kJ/mol for chemical adsorptions [96]. In this study, the ΔG^o values ranged from –2.08 to –4.74 kJ/mol, which indicates that biosorption is mainly physical. The negative ΔH^o value (–44.37 kJ/mol) confirms that the biosorption is exothermic in nature. The type of biosorption process can also be explained in terms of the magnitude of ΔH^o. The heat evolved during physisorption generally lies in the range of 2.1 to 20.9 kJ/mol while the heat of chemisorption falls into a range of 80 to 200 kJ/mol [97]. The enthalpy value of 44.37 kJ/mol obtained in this study is lower than the range for chemisorption but is closer to the range for physisorption, which suggests that the biosorption process is more of a physisorption. The result is consistent with those obtained from the Temkin and Dubinin–Radushkevich isotherms. This may probably be due to the fact that physisorption, which is as a result of weak Van der Waal forces between the sorbate and the biosorbent, occurs at low temperatures and decreases with increase in temperature [98].

The negative value of ΔS^o is an indication of the decreasing randomness of 2,4-DNP molecules and also suggests that the biosorption process is irreversible and enthalpy-driven [1]. The E_a value calculated from the slope of the plot (Figure 14b) was found to be –17.26 kJ/mol. The negative value of E_a indicates that lower solution temperature favors organic chemical removal by biosorption onto the chemically treated kola nut pod surface and that the biosorption process is exothermic in nature. The magnitude of the activation energy (E_a) can give an idea about the type of biosorption, which is mainly physical or chemical [99]. Physisorption usually has activation energies (E_a) in the range of 5 to 40 kJ/mol, while higher activation energies (E_a) of 40 to 800 kJ/mol suggest chemisorption [100]. In this study, the value of E_a is less than 40 kJ/mol, which suggests that the biosorption process is physisorption.

3.9. Design of batch biosorption from isotherm data

For the biosorption of 2,4-DNP by chemically treated kola nut pod, the Sips isotherm gives the best fit to experimental data. Therefore, to design a batch biosorption process, where the effluent contains V (L) of water and an initial 2,4-DNP concentration C_0, which is to be reduced to C_1 in the biosorption process, Eq. (29) can be applied.

$$\frac{W}{V} = \frac{C_0 - C_1}{q_e} = \frac{C_0 - C_e}{Q_S a_S C_e^{\beta_S} / 1 + a_S C_e^{\beta_S}} \tag{29}$$

Figure 15 shows a series of plots (70%, 80%, and 90% 2,4-DNP removal at different solution volumes, i.e. 1, 2, 3, 4, and 5 L) derived from Eq. (29) for the biosorption of 2,4-DNP by chemically treated kola nut pod at an initial concentration of 100 mg/L. The amount of chemically treated kola nut pod required for the 90% removal

of 2,4-DNP solution of concentration 100 mg/L was 26.6, 53.2, 79.8, 106.04, and 133 g for 2,4-DNP solution volumes of 1, 2, 3, 4, and 5 L, respectively.

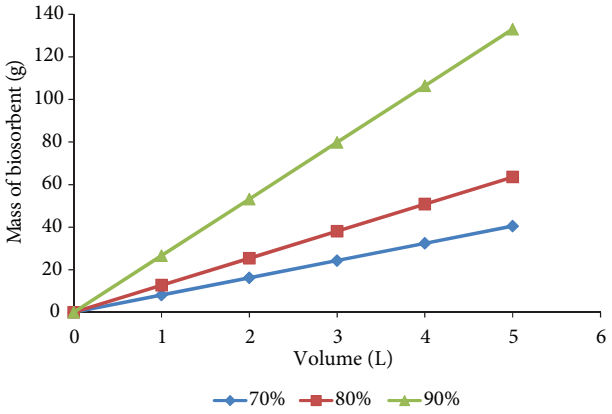

Figure 15. Mass of biosorbent (g) against volume of effluent (L) treated for different percentages of 2,4-DNP removal (C_o = 100 mg/L).

4. Conclusions

In this study, chemically treated kola nut pod was tested and evaluated as a possible biosorbent for removal of 2,4-DNP from aqueous solution using batch biosorption techniques. The biosorption process is also dependent on some factors such as the initial concentration, contact time, biosorbent particle size, pH, temperature, and biosorbent dosage. The percentage removal of 2,4-DNP decreased with an increase in the initial 2,4-DNP concentration while it increased with increase in contact time and biosorbent dose up to a certain level. A detailed error analysis was carried out to determine the best isotherm model for equilibrium biosorption data of 2,4-DNP onto chemically treated kola nut pod. Among the 2- and 3-parameter isotherm models examined, the Langmuir and Sips isotherm model equations showed the best fit to the equilibrium biosorption data based on lower SNE values. In general, the Sips isotherm equation employing the parameter set derived using the HYBRID/MPSD/ARE errors provided the overall best model for the experimental system. The maximum monolayer biosorption capacity ($Q_{\max}$) was found to be 32.26 mg/g with linear regression and 30.10 mg/g with nonlinear regression. The biosorption kinetics followed a pseudo-first-order kinetic model with a very good correlation coefficient, suggesting that the biosorption process is presumable a physisorption. Intraparticle diffusion was not the sole rate-controlling factor. The activation energy of the biosorption process (E_a) was found to be –17.26 kJ/mol by using the Arrhenius equation, indicating the exothermic nature of 2,4-DNP biosorption onto chemically treated kola nut pod.

Thermodynamic analysis suggests that the removal of 2,4-DNP from aqueous solution by chemically treated kola nut pod was a spontaneous and exothermic process. Negative values for ΔG^o, ΔH^o, and E_a indicated that biosorption occurs in a spontaneous and exothermic manner, while the negative value of ΔS° indicated decreasing disorder at the solid/solution interface during biosorption. In addition, values of the standard enthalpy change (ΔH^o) and activation energy (E_a) suggested that the biosorption process of 2,4-DNP onto chemically treated kola nut pod might be of the physisorption process.

References

[1] Varank, G, Demir A, Yetilmezsoy K, Top S, Sekman E, Bilgili MS. Removal of 4-nitrophenol from aqueous solution by natural low-cost adsorbents. Indian J Chem Technol 2012; 19: 7–25.

[2] Marais E, Nyokong T. Adsorption of 4-nitrophenol onto Amberlite®IRA-900 modified with metallophthalocyanines. J Hazard Mater 2008; 152: 293–301.

[3] Soni A, Tiwari A, Bajpai AK. Adsorption of o-nitrophenol onto nano iron oxide and alginate microspheres: batch and column studies. African Journal of Pure and Applied Chemistry 2012; 6: 161–173.

[4] Goncharuk VV, Kucheruk DD, Kochkodan VM, Badekha VP. Removal of organic substances from aqueous solution by reagent enhanced reverse osmosis. Desalination 2002; 143: 45–51.

[5] Acero JL, Benitez FJ, Leal AI, Real FJ. Removal of phenolic compounds in water by ultrafiltration membrane treatments. J Environ Sci Heal A 2005; 40: 1585–1603.

[6] Canizares P, Lobato J, Paz R, Rodrigo MA, Saez C. Electrochemical oxidation of phenolic wastes with boron-doped diamond anodes. Water Res 2005; 39: 2687–2703.

[7] Roostaei N, Tezel FH. Removal of phenol from aqueous solutions by adsorption. J Environ Manage 2004; 70: 157–164.

[8] Poulopoulos SG, Arvanitakis F, Philippopoulos CJ. Photochemical treatment of phenol aqueous solutions using ultraviolet radiation and hydrogen peroxide. J Hazard Mater 2006; 129: 64–68.

[9] Banat AF, Al-Bashir B, Bal-Asheh S, Hayajineh O. Adsorption of phenol by bentonite. Environ Pollut 2000; 107: 391–398.

[10] Pandey PK, Sharma SK, Sambi SS. Kinetics and equilibrium studies of chromium adsorption on zeolite NaX. Int J Environ Sci Tech 2010; 7: 395–404.

[11] Mackay AA, Gschwend PM. Sorption of monoaromatic hydrocarbons to wood. Environ Sci Technol 2000; 34: 839–845.

[12] Coruh S, Geyikci F, Ergun ON. Adsorption of basic dye from wastewater using raw and activated red mud. Environ Technol 2011; 32: 1183–1193.

[13] Crisafully R, Milhome MA, Cavalcante RM, Silveira ER, Keukeleire D, Nascimento F. Removal of some polycyclic aromatic hydrocarbons from petrochemical wastewater using low-cost adsorbents of natural origin. Bioresour Technol 2008; 99: 4515–4519.

[14] Popuri SR, Jammala A, Reddy KVN, Abburi K. Biosorption of hexavalent chromium using tamarind (*Tamarindus indica*) fruit shell: a comparative study. Electron J Biotechnol 2007; 3: 358–367.

[15] Li X, Tang Y, Cao X, Lu D, Luo F, Shao W. Preparation and evaluation of orange peel cellulose adsorbents for effective removal of cadmium, zinc, cobalt and nickel. Colloids Surf 2008; A317: 512–521.

[16] Li Y, Chen B, Zhu L. Enhanced sorption of polycyclic aromatic hydrocarbons from aqueous solution by modified pine bark. Bioresour Technol 2010; 101: 7307–7313.

[17] Almeida JL, Antoniosi NR, Alves MIR, Carvalho BG, Melo NM. Removal of BTEX from aqueous solution using *Moringa oleifera* seed cake. Environ Technol 2012; 33: 1299–1305.

[18] Agarry SE, Ogunleye OO, Aworanti OA. Biosorption equilibrium, kinetic and thermodynamic modelling of naphthalene removal from aqueous solution onto modified spent tea leaves. Environ Technol 2013; 34: 825–839.

[19] Ho YS, Porter JF, Mckay G. Equilibrium isotherm studies for the sorption of divalent metal ions onto peat: copper, nickel and lead single component systems. Water Air Soil Poll 2002; 141: 1–33.

[20] Vijayaraghavan K, Padmesh TVN, Palanivelu K, Velan M. Biosorption of nickel(II) ions onto *Sargassum wightii*: application of two-parameter and three-parameter isotherm models. J Hazard Mater 2006; 133: 304–308.

[21] Sathishkumar M, Binupriya AR, Kavitha D, Selvakumar R, Jayabalan R, Choi JG, Yun SE. Adsorption potential of maize cob carbons for 2,4-dichlorophenol removal from aqueous solutions: equilibrium, kinetics and thermodynamic modeling. Chem Eng J 2009; 147: 265–271.

[22] Bailey SE, Olin TJ, Bricka RM, Adrian DD. A review of potentially low-cost sorbents for heavy metals. Water Res 1999; 33: 2469–2479.

[23] Lavecchia R, Pugliese A, Zuorro A. Removal of lead from aqueous solutions by spent tea leaves. Chem Eng Trans 2010; 19: 73–78.

[24] Yaneva Z, Koumanova B. Comparative modeling of mono and dinitrophenols sorption on yellow bentonite from aqueous solutions. J Colloid Interface Sci 2006; 293: 303–311.

[25] Chen S, Xu ZP, Zhang Q, Max Lu GQ, Hao ZP, Liu S. Studies on adsorption of phenol and 4-nitrophenol on MgAl-mixed oxide derived from MgAl-layered double hydroxide. Sep Purif Technol 2009; 67: 194–200.

[26] Oludemokun AA. Processing, storage and utilization of kolanuts, *Cola nitida* and *Cola acuminata.* Trop Sci 1983; 24: 111–117.

[27] Brickell C, Cole CT, Cathey HM. The American Horticultural Society Encyclopedia of Plants and Flowers. New York, NY, USA: D.K. Publishing; 2002.

[28] Oladokun MAO. Morpho-physiological aspect of germination, rooting and seedling growth in kola. PhD, University of Ibadan, Ibadan, Nigeria, 1982.

[29] Oguntuga DBA. Chemical composition and potential commercial uses of kola nuts, *Cola nitida* (Vent) Schoot & Endlicher. Ghana J Agric Sci 1975; 8: 121–125.

[30] Jayeola CO. Preliminary studies on the use of kolanuts (*Cola nitida*) for soft drink production. Journal of Food Technology in Africa 2001; 6: 25–26.

[31] Omojola MO, Akinkunmi YO, Olufunsho KO, Egharevba HO, Martins EO. Isolation and physical-chemical characterization of cola starch. Afri J Food Agric Nutr Dev 2010; 10: 2884–2900.

[32] Nunes CA, Guerreiro MC. Estimation of surface area and pore volume of activated carbons by methylene blue and iodine numbers. Quim Nova 2011; 34: 472–476.

[33] Bajpai SK, Tankhiwale R. Preparation, characterization and preliminary calcium release study of floating sodium alginate/dextran-based hydrogel beads: Part I. Polym Int 2008; 57: 57–65.

[34] Saha P, Sanyal SK. Assessment of the removal of cadmium present in wastewater using soil-admixture membrane. Desalination 2010; 259: 131–139.

[35] Yuan X, Zhuo SP, Xing W, Cui HY, Dai XD, Liu XM, Yan ZF. Aqueous dye adsorption on ordered malodorous carbons. J Colloid Interface Sci 2007; 310: 83–89.

[36] Hamad BK, Noor AM, Rahim AA. Removal of 4-chloro-2-methoxyphenol from aqueous solution by adsorption to oil palm shell activated carbon activated with K_2CO_3. J Phys Sci 2011; 22: 39–55.

[37] Ahmed MJ, Theydan SK, Mohammed AAK. Adsorption of phenol and p-nitro phenol onto date stones: equilibrium isotherms, kinetics and thermodynamics studies. J Eng 2012; 18: 743–761.

[38] Onundi YB, Mamun AA, Al Khatib MF, Suleyman AM. Heavy metals removal from synthetic wastewater by a novel nano-size composite adsorbent. Int J Environ Sci Technol 2011; 8: 799–806.

[39] Agarry SE, Owabor CN, Ajani AO. Modified plantain peel as cellulose-based low-cost adsorbent for the removal of 2,6-dichlorophenol from aqueous solution: adsorption isotherms, kinetic modelling and thermodynamic studies. Chem Eng Comm 2013; 200: 1121–1147.

[40] Tsai WT, Chen HR. Removal of malachite green from aqueous solution using low-cost chlorella-based biomass. J Hazard Mater 2010; 175: 844–849.

[41] Baek MH, Ijagbemi CO, Se-Jin O, Kim DS. Removal of malachite green from aqueous solution using degreased coffee bean. J Hazard Mater 2010; 176: 820–828.

[42] Potgieter JH, Bada SO, Potgieter-Vermaak SS. Adsorptive removal of various phenols from water by South African coal fly ash. Water SA 2009; 35: 89–96.

[43] Alinnor IJ, Nwachukwu MA. A study on removal characteristics of para-nitrophenol from aqueous solution by fly ash. J Environ Chem Ecotoxicol 2011; 3: 32–36.

[44] Annadurai A, Babu SR, Mahesh KPO, Murugesan T. Adsorption and biodegradation of phenol by chitosan immobilized *Pseudomonas putida* (NICM 2174). Bioprocess Biosyst Eng 2000; 2: 493–501.

[45] Agarry SE, Aremu MO. Batch equilibrium and kinetic studies of simultaneous adsorption and biodegradation of phenol by pineapple peels immobilized *Pseudomonas aeruginosa* NCIB 950. British Biotechnology Journal 2012; 2: 26–48.

[46] Dabhade, MA, Saidutta MB, Murthy DVR. Adsorption of phenol on granular activated carbon from nutrient medium: equilibrium and kinetic study. Int J Environ Res 2009; 3: 557–568.

[47] Al-Aoh HA, Maah MJ, Ahmad AA, Bin Abas MR. Isotherm and kinetic studies of 4-nitrophenol adsorption by NaOH-modified palm oil fuel ash. J Purit Util React Environ 2012; 1: 104–120.

[48] Ahmaruzzaman M, Gayatri SL. Batch adsorption of 4-nitrophenol by acid activated jute stick char: equilibrium, kinetic and thermodynamic studies. Chem Eng J 2010; 158: 173–180.

[49] Bhatgava DS, Sheldarkar SB. Adsorption of para-nitrophenol on clay. Water Res 1993; 27: 313.

[50] Savova D, Apak E, Ekinci E, Yardim F, Petrof N, Budinova T, Razvigorova M, Minikora V. Biomass conversion to carbon adsorbents and gas. Biomass Bioenerg 2001; 21: 133–142.

[51] Crini G, Peindy HN, Gimbert F, Robert C. Removal of C.I. Basic Green 4 (Malachite Green) from aqueous solutions by adsorption using cyclodextrin based adsorbent: kinetic and equilibrium studies. Sep Purif Technol 2007; 53: 97–110.

[52] Akar ST, Ozcan AS, Akar T, Ozcan A, Kaynak Z. Biosorption of a reactive textile dye from aqueous solutions utilizing an agro-waste. Desalination 2009; 249: 757–761.

[53] Gok A, Ozcan S, Ozcan A. Adsorption kinetics of naphthalene on to organo-sepiolite from aqueous solutions. Desalination 2008; 220: 96–107.

[54] Das B, Mondal NK. Calcareous soil as a new adsorbent to remove lead from aqueous solution: Equilibrium, kinetic and thermodynamic study. Univer J Environ Res Technol 2011; 1: 515–530.

[55] Nasuha N, Hameed BH, Din ATM. Rejected tea as a potential low cost adsorbent for the removal of methylene blue. J Hazard Mater 2010; 175: 126–132.

[56] McKay G, Allen SJ, McConvey IF. The adsorption of dyes from solution – equilibrium and column studies. Water Air Soil Poll 1984; 21: 127–129.

[57] Ratkowski DA. Handbook of Nonlinear Regression Models. New York, NY, USA: Marcel Dekker; 1990.

[58] Malek A, Farooq S. Comparison of isotherm models for hydrocarbon adsorption on activated carbon. AIChE J 1996; 42: 431–441.

[59] Perez-Marin AB, Meseguer Zapata V, Ortuno JF, Aguilar M, Saez J, Llorens M. Removal of cadmium from aqueous solutions by adsorption onto orange waste. J Hazard Mater 2007; 136: 122–131.

[60] Yaneva ZL, Koumanova BK, Georgieva NV. Linear and non-linear regression methods for equilibrium modelling of p-nitrophenol biosorption by *Rhizopus oryzae*: comparison of error analysis criteria. Journal of Chemistry 2013; 2013: 51763.

[61] Langmuir I. The adsorption of gases on plane surfaces of glass, mica and platinum. J Am Chem Soc 1918; 40: 1361–1368.

[62] Chen Z, Ma W, Han M. Biosorption of nickel and copper onto treated alga (*Undaria pinnarlifida*): application of isotherm and kinetic models. J Hazard Mater 2008; 155: 327–333.

[63] Ofomaja AE. Kinetics and pseudo-isotherm studies of 4-nitrophenol adsorption onto mansonia wood sawdust. Ind Crop Prod 2011; 33: 418–428.

[64] Li JM, Meng XG, Hu GW, Du J. Adsorption of phenol, p-chlorophenol and p-nitro phenol onto functional chitosan. Bioresour Technol 2009; 100: 1168–1173.

[65] Hall KR, Eagleton LC, Axerivos A, Vermeuleu T. Pore and solid diffusion kinetics in fixed bed adsorption under constant pattern conditions. Ind Eng Chem Res 1966; 212–216.

[66] Annadurai G, Chellapandian M, Krishnan MRV. Adsorption of basic dye from aqueous solution by chitosan: equilibrium studies. Indian J Environ Prot 1997; 17: 95–98.

[67] Anirudhan TS, Radhakrishnan PG. Thermodynamics and kinetics of adsorption of Cu (II) from aqueous solutions onto a new cation exchanger derived from tamarind fruit shell. J Chem Thermodyn 2008; 40: 702–709.

[68] Freundlich HMF. Over the adsorption in solution. J Phys Chem 1906; 57: 385–471.

[69] McKay G, Blair HS, Gardner JR. Adsorption of dyes on chitin I: equilibrium studies. J Appl Polym Sci 1982; 27: 3043–3057.

[70] Treybal RE. Mass Transfer Operation. 2nd ed. New York, NY, USA: McGraw-Hill; 1988.

[71] Redlich O, Peterson DLA. Useful adsorption isotherm. J Phys Chem 1998; 63: 1024–1029.

[72] Sathishkumar M, Binupriya AR, Vijayaraghavan K, Yun SI. Two and three-parameter isothermal modeling for liquid-phase sorption of Procion Blue H-B by inactive mycelial biomass of *Panus fulvus*. J Chem Technol Biotechnol 2007; 82: 389–398.

[73] Padmesh TVN, Vijayaraghavan K, Sekaranb G, Velan M. Application of two- and three-parameter isotherm models: biosorption of acid red 88 onto *Azolla microphylla*. Bioremediation J 2006; 10: 37–44.

[74] Mane VS, Mall ID, Srivastava VC. Kinetic and equilibrium isotherm studies for the adsorptive removal of Brilliant Green dye from aqueous solution by rice husk ash. J Environ Manage 2007; 84: 390–400.

[75] Sips R. Combined form of Langmuir and Freundlich equations. J Chem Phys 1971; 16: 490–495.

[76] Foo KY, Hameed BH. Insights into the modelling adsorption isotherm systems. Chem Eng J 2010; 156: 2–10.

[77] Ncibi MC. Applicability of some statistical tools to predict optimum adsorption isotherm after linear and non-linear regression analysis. J Hazard Mater 2008; 153: 207–212.

[78] Chang CF, Chang CY, Chen KH, Tsai WT, Shie JL, Chen YH. Adsorption of naphthalene on zeolite from aqueous solution. J Colloid Interface Sci 2004; 277: 29–34.

[79] Lagergren S. Zur theorie der sogenannte adsorption gelöster stoffe. Kungliga Svenska vetenskapsakademiens Handlingar 1898; 24: 1–39 (in German).

[80] Ho YS, McKay G. The kinetics of sorption of divalent metal ions onto sphagnum moss peat. Water Res 2000; 34: 735–742.

[81] Low MJO. Kinetics of chemisorptions of gases on solids. Chem Rev 1960; 60: 267–312.

[82] Goswami S, Ghosh UC. Different bioadsorbents capacity to uptake impurity from wastewater. Water SA 2005; 31: 597–560.

[83] Weber WJ, Morris JC. Kinetics of adsorption on carbon from solution. J Sanit Eng Div Am Soc Civ Eng 1963; 89: 31–60.

[84] Ho YS, McKay G. The sorption of lead(II) ions on peat. Water Res 1999; 33: 578–584.

[85] Štrkalj A, Malina J. Thermodynamic and kinetic study of adsorption of Ni(II) ions on carbon anode dust. Chem Eng Comm 2011; 198: 1497–1504.

[86] Sari A, Citak D, Tuzen M. Equilibrium, thermodynamic and kinetic studies on adsorption of Sb(III) from aqueous solution using low-cost natural diatomite. Chem Eng J 2010; 162: 521–527.

[87] Hameed BH, Mahmoud DK, Ahmad AL. Equilibrium modeling and kinetic studies on the adsorption of basic dye by a low-cost adsorbent: coconut (*Cocos nucifera*) bunch waste. J Hazard Mater 2008; 158: 65–72.

[88] Chien SH, Clayton WR. Application of Elovich equation to the kinetics of phosphate release and sorption in soils. Am J Soil Sci Soc 1980; 44: 265–268.

[89] Sparks DL. Kinetics and mechanisms of chemical reactions at the soil mineral/water interface. In: Sparks DL, editor. Soil Physical Chemistry. Boca Raton, FL, USA: CRC Press; 1999. pp. 135–192.

[90] Chingombe P, Saha B, Wakeman RJ. Sorption of atrazine on conventional and surface modified activated carbons. J Colloid Interface Sci 2006; 302: 408–416.

[91] Ozcan A, Ozcan AS, Gok O. Adsorption kinetics and isotherms of anionic dye of reactive blue 19 from aqueous solutions onto DTMA-sepiolite. In: Lewinsky AA, editor. Hazardous Materials and Wastewater—Treatment, Removal and Analysis. New York, NY, USA: Nova Science Publishers; 2007. pp. 225–249.

[92] Unuabonah EI, Adebowale KO, Olu-Owolabi BI. Kinetic and thermodynamic studies of the adsorption of lead (II) ions onto phosphate-modified kaolinite clay. J Hazard Mater 2007; 144: 386–395.

[93] Koyuncu H. Adsorption kinetics of 3-hydroxybenzaldehyde on native and activated bentonite. Appl Clay Sci 2008; 38: 279–287.

[94] Wu FC, Tseng RL, Juang RS. Initial behavior of intraparticle diffusion model used in the description of adsorption kinetics. Chem Eng J 2009; 153: 1–8.

[95] Boyd GE, Adamson AW, Myers LS. The exchange adsorption of ions from aqueous solutions by organic zeolites II, kinetics. J Am Chem Soc 1947; 69: 2836–2848.

[96] Yu Y, Zhuang YY, Wang ZH, Qiu MQ. Adsorption of water-soluble dyes onto modified resin. Chemosphere 2004; 54: 425–430.

[97] Liu Y, Liu YJ. Biosorption isotherms, kinetics and thermodynamics. Sep Purif Technol 2008; 61: 229–242.

[98] Itodo AU, Itodo HU. Sorption energies estimation using Dubinin-Radushkevich and Temkin adsorption isotherms. Life Sci J 2010; 7: 31–39.

[99] Chen AH, Chen SM. Biosorption of azo dyes from aqueous solution by glutaraldehyde-crosslinked chitosans. J Hazard Mater 2009; 172: 1111–1121.

[100] Hameed BH, Ahmad AA, Aziz N. Isotherms, kinetics and thermodynamics of acid dye adsorption on activated palm ash. Chem Eng J 2007; 133: 195–203.